iScience

Article

Miscompartmentalization of microbiota-derived TMAO is a reversible driver in autism spectrum disorder

Graphical abstract

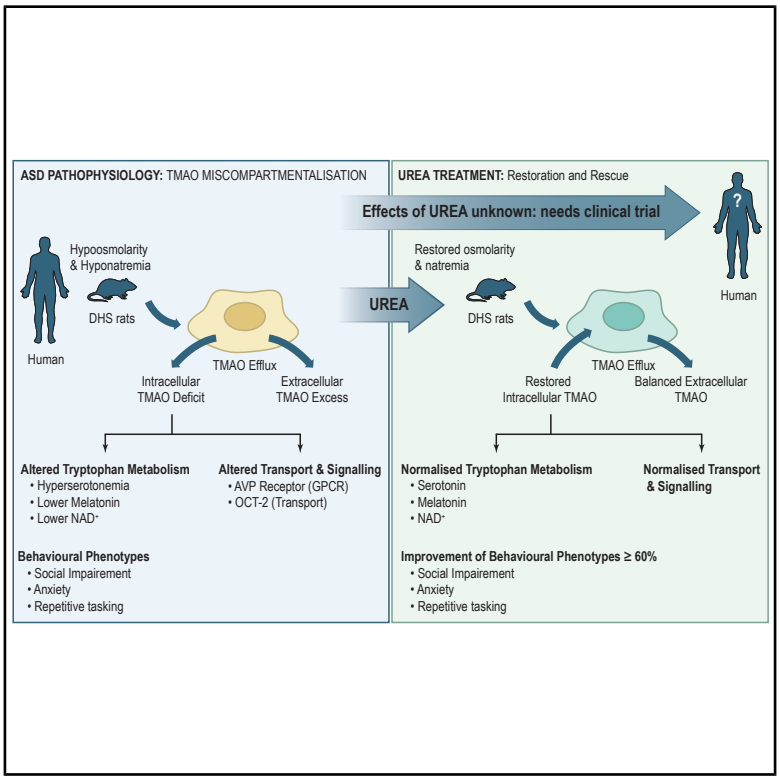

Highlights

- ASD is characterized my several biochemical anomalies
- TMAO chaperones numerous enzymatic reactions and is miscompartmentalized in ASD
- Urea restored TMAO compartmentalization in a rat model of ASD
- Urea restored biochemical anomalies and improved behavior in a rat model of ASD

Authors

Jean-Marie Launay, Nicolas Vodovar

Correspondence

jean-marie.launay@inserm.fr (J.-M.L.), nicolas.vodovar@inserm.fr (N.V.)

In brief

Health sciences; Medicine; Medical specialty; Internal medicine; Neurology; Natural sciences; Biological sciences; Neuroscience; Behavioral neuroscience

Launay & Vodovar, 2026, iScience *29*, 117276
September 18, 2026
https://doi.org/10.1016/j.isci.2026.117276

CellPress

iScience

CellPress
OPEN ACCESS

Article

Miscompartmentalization of microbiota-derived TMAO is a reversible driver in autism spectrum disorder

Jean-Marie Launay[1,*] and Nicolas Vodovar[1,2,*]
[1]Université Paris Cité and Inserm UMR-S 942 MASCOT, Paris, France
[2]Lead contact
*Correspondence: jean-marie.launay@inserm.fr (J.-M.L.), nicolas.vodovar@inserm.fr (N.V.)
https://doi.org/10.1016/j.isci.2026.117276

SUMMARY

Autism spectrum disorder (ASD) is a heterogeneous neurodevelopmental disorder. Unlike genetics and gut dysbiosis, ASD appears to be homogeneous when considering tryptophan metabolism. Following these findings, we found that ASD was associated with the miscompartmentalization of the chemical chaperone trimethylamine *N*-oxide (TMAO). Intracellular TMAO was markedly reduced in ASD, possibly due to altered fluid/electrolyte homeostasis, which appeared to be responsible for most anomalies of tryptophan metabolism described in ASD. Administration of urea in a rat model of ASD that recapitulates the biochemical and behavioral phenotypes observed in humans not only restored biochemical parameters but also broadly improved behaviors. Our results suggest a major role of TMAO miscompartmentalization in the pathophysiology of ASD, although it is not causal for ASD. We anticipate that urea, which is already clinically approved, offers a new therapeutic opportunity for ASD, although careful testing is required to ensure safety and acceptability in this context.

INTRODUCTION

ASD is a complex and heterogeneous neurodevelopmental disorder characterized by impaired social communication, restrictive interest, repetitive behaviors, and hypersensitivity.[1] To date, there is no broadly effective treatment for ASD. Although genetic factors have been associated with ASD,[2–4] at most 10% of cases can be attributed to specific mutations, and >1,000 genetic variants have been associated with ASD.[4] Gut dysbiosis has also been associated with the severity of mental illness[5] and has been proposed as a driving factor in ASD, although dysbiosis appears more as a consequence than a cause of ASD.[6] From a metabolic standpoint, ASD is characterized by numerous biochemical alterations, particularly in tryptophan (Trp) metabolism. These alterations include reduced enzymatic activities related to serotonin (5-HT) catabolism by sulphoconjugation[7] and the synthesis of melatonin,[8] kynurenines, and nicotinamide adenine dinucleotide (NAD^+).[9] In marked contrast to genetics and microbiota findings, our recent findings suggest that ASD is metabolically more homogeneous than initially thought.[9]

Trimethylamine *N*-oxide (TMAO) is the oxidation product of trimethylamine (TMA), which is produced by the gut microbiota, by liver flavin-containing monooxygenase 3 (FMO3).[10] TMAO is a chemical chaperone that facilitates protein folding[11–14] and prevents protein denaturation by urea[15] and hydrostatic pressure in marine animals.[16] TMAO also stabilizes the tertiary structure of RNA *in vitro*[17] and increases the rigidity of lipid membranes.[18–21] More recently, elevated TMAO plasma levels have been associated with cardiometabolic diseases,[22–24] and a study has reported elevated plasma TMAO levels in ASD.[25]

Here, we first identified TMAO as a chemical chaperone involved in melatonin synthesis and described the miscompartmentalization of TMAO (extracellular excess and intracellular deficit) in individuals with ASD. Second, we found that other biochemical anomalies observed in ASD[7,9] are also dependent on TMAO. Third, we found that TMAO miscompartmentalization in ASD likely resulted from altered osmolarity, and we finally successfully corrected TMAO miscompartmentalization with urea in a preclinical model of ASD with biochemical and behavioral benefits.

RESULTS

Intracellular TMAO is lower in ASD

Melatonin is produced from 5-HT by the sequential action of arylalkylamine N-acetyltransferase (AANAT) and acetylserotonin O-methyltransferase (ASMT), whose activities are reduced in ASD.[8] The activity of both enzymes depends on the 14-3-3 chaperone, whose levels are also reduced in ASD.[8] AANAT activity[26] was more sensitive than ASMT activity to 14-3-3 levels,[8] which is reflected by the strong positive correlation between platelet 14-3-3 concentration and platelet AANAT activity, only in individuals with ASD (Figure 1A) and the lack thereof for platelet ASMT activity (Figure 1B). However, a decrease in ASMT activity without any decrease in AANAT activity was

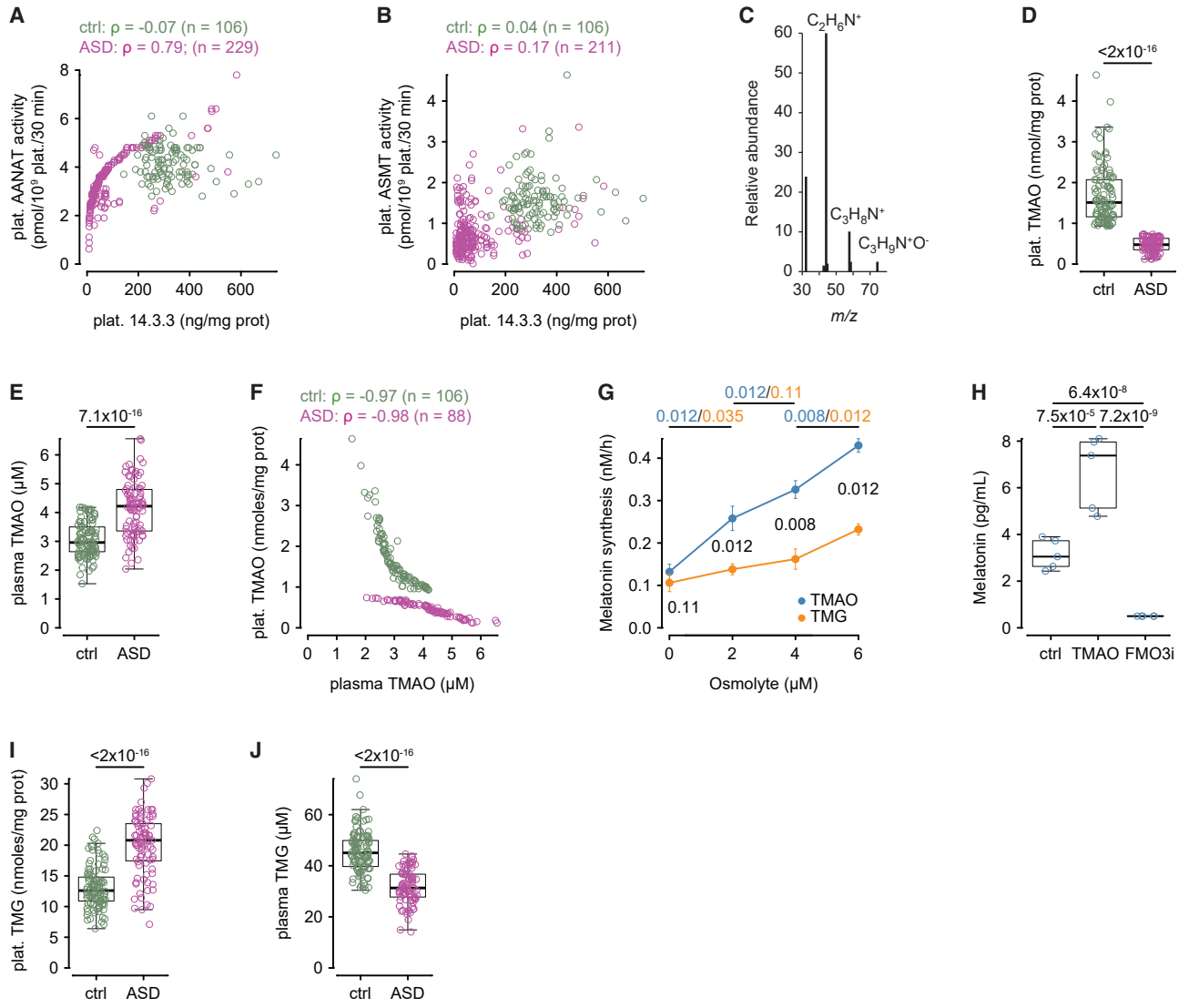

Figure 1. TMAO chaperones melatonin synthesis

(A) Relationship between platelet 14-3-3 concentration and platelet AANAT activity measured in the platelets of controls and individuals with ASD.
(B) Relationship between platelet 14-3-3 concentration and platelet ASMT activity measured in the platelets of controls and individuals with ASD.
(C) Representative GC/MS spectrum obtained from platelet AANAT or ASMT immunoprecipitates of healthy individuals.
(D) Platelet TMAO concentration in controls (n = 106) and individuals with ASD (n = 88).
(E) Plasma TMAO concentration in controls (n = 106) and individuals with ASD (n = 88).
(F) Relationship between plasma and platelet TMAO concentrations in controls and individuals with ASD.
(G) *In vitro* melatonin synthesis by recombinant human AANAT, ASMT and 14-3-3 with respect to TMAO concentration (n = 5 per osmolyte concentration).
(H) Melatonin plasma levels in control mice, that successively received TMAO and FMO3 inhibitor (n = 5 per group, see methods).
(I) Platelet concentration of trimethyl glycine (TMG) in controls (n = 105) and individuals with ASD (n = 66).
(J) Plasma TMG concentration in controls (n = 106) and individuals with ASD (n = 88).
Data are presented as mean ± SD (G) or as median and interquartile range along with individual datapoints (D, E, H, I, and J). Intergroup comparisons were performed using the Wilcoxon sum-rank test (D, E, I, and J) or the Kruskal-Wallis test followed by the Wilcoxon sum-rank test corrected for multiple comparisons (G). Within-group comparisons were performed using repeated-measure ANOVA on log-transformed data, followed by the Tukey HSD test (H). Correlations (A, C, and F) were calculated using Spearman's correlation coefficient (ρ). The corresponding p values are presented in Table S1. The number of individuals for each correlation is indicated on each plot.

observed in ~41% of individuals with ASD,[8] suggesting that another chaperone could be involved. Therefore, we immunoprecipitated AANAT or ASMT from 50 × 10^9 platelets from healthy subjects (n = 6) and subjected the immunoprecipitates to native mass spectrometry.[27] Regardless of the antigen targeted, the immunoprecipitates always contained AANAT, 14-3-3, and ASMT, indicating that the three proteins formed a complex *in vivo*. We also subjected the immunoprecipitates to

GC-MS and consistently found three peaks (m/z = 75, 58, and 44), which were identified as TMAO and its fragmentation products (Figure 1C). Of note, this finding is consistent with a recent report that TMAO interacts with 14-3-3.[28] Next, we quantified the concentration of TMAO in platelets and plasma of individuals with ASD and controls from the same cohort in which we described various anomalies in tryptophan metabolism.[7,9,29] Platelet TMAO was markedly lower (Figure 1D), while plasma TMAO was higher (Figure 1E) in individuals with ASD, with strong correlations between plasma and platelet TMAO in individuals with ASD and controls (Figure 1F), indicating that TMAO is miscompartmentalized in ASD. TMAO miscompartmentalization did not result from a deficit in TMAO synthesis since whole blood levels of TMAO (Figure S1A) and those of its gut microbiota-derived precursor, TMA (Figure S1B), were 26.8% and 14.8% higher in individuals with ASD compared to controls, respectively. To functionally test the role of TMAO in melatonin synthesis, we measured melatonin production *in vitro* by incubating 5-HT with human recombinant AANAT, ASMT, and 14-3-3 along with increasing TMAO concentrations, and found that melatonin synthesis increased with increasing TMAO concentrations (Figure 1G). These results were confirmed *in vivo*, as in male mice (FVB/N), the administration of TMAO (50 mg/kg) caused a parallel increase in platelet and plasma TMAO (Figures S1C and S1D), and plasma melatonin (Figure 1H), while the administration of an FMO3 inhibitor (phenylthiourea 3 mg/kg, FMO3i) to inhibit TMAO synthesis decreased platelet and plasma TMAO (Figures S1C and S1D), and plasma melatonin (Figure 1H).

Finally, to test the specificity of TMAO with respect to melatonin synthesis, we evaluated the impact of another osmolyte known to modulate enzymatic activities, trimethyl glycine (TMG, glycine betaine, betaine). *In vitro*, TMG had modest effects on melatonin synthesis compared to TMAO (Figure 1G). Furthermore, platelet TMG concentrations were higher (Figure 1I) and plasma TMG levels were lower (Figure 1J) in individuals with ASD, when compared to controls. There was no relationship between platelet and plasma TMG in either group (Figure S1E).

Taken together, these data suggest that TMAO miscompartmentalization in ASD is responsible for the decrease in AANAT/ASMT/14.3.3 chaperoning by TMAO, hence a reduction in melatonin production.

TMAO and other Trp metabolism alterations in ASD

The eukaryotic Trp metabolic pathways (Figure 2A) are markedly altered in ASD. In addition to deficits in melatonin synthesis[8] and sulphoconjugation (monoamine-specific phenol sulfotransferase, PST-M and phenol-specific phenol sulfotransferase, PST-P),[7] a decrease in 3-hydroxyanthranilate oxidase (3-HAO) activity, which resulted in the accumulation of 3-hydroxyanthranilate (3-HAA), and a deficit in NAD^+ production were reported.[9] As TMAO is a chemical chaperone, and based on the principle of parsimony, we tested the role of TMAO on these enzymes *in vitro* and *in vivo*. First, human recombinant PST-P activity increased with increasing TMAO concentrations added to the reaction buffer (Figure 2B) and platelet PST (the sole PST in rodents) activity was unaffected by TMAO administration but decreased when TMAO synthesis was blocked by FMO3i in mice (Figure 2C). Second, 3-HAO activity, estimated by the ratio of plasma quinolinic (QA) + picolinic acids (PA) to 3-HAA (Figure 2A), was strongly negatively and negatively correlated with plasma (Figure 2D) and platelet (Figure S2A) TMAO, respectively, only in individuals with ASD. *In vitro*, the activity of human recombinant 3-HAO increased with increasing TMAO concentrations added to the reaction buffer (Figure 2E), and *in vivo,* exogenous TMAO increased while FMO3i decreased liver 3-HAO activity (Figure 2F). Finally, plasma NAD^+ concentrations negatively and positively correlated with plasma (Figure 2G) and platelet (Figure S2B) TMAO, respectively, only in individuals with ASD and NAD^+ plasma levels increased after TMAO administration and decreased after FMO3 inhibition in mice (Figure 2H). Of note, both PST-P and 3-HAO activities increased *in vitro* after the addition of TMG (Figures 2B–2E), albeit to a lesser extent than when TMAO was added. Taken together, these results strongly suggest that TMAO chaperones different enzymatic processes that were found to be altered ASD.[7–9]

Osmolarity and TMAO intracellular depletion

TMAO can be released from cells as a compatible solute to compensate for a decrease in extracellular osmolarity.[30,31] In our cohort, the only osmolarity-related parameter available was natremia, and we found that 81% (n = 73/90) of individuals with ASD were hyponatremic (<135 mM, Figure 3A). Furthermore, there were strong correlations between natremia, platelet (Figure 3B), and plasma (Figure 3C) TMAO concentrations in individuals with ASD, especially in hyponatremic individuals. To confirm the role of osmolarity in TMAO compartmentalization, we resuspended fresh human platelets from healthy controls in Tyrode solutions at different osmolarities and measured TMAO in the platelets and the supernatant. At 300 mOsm/L, there was no detectable TMAO release, while TMAO was released in a dose-response fashion at lower osmolarities (Figure 3D). To confirm the functional impact of osmolarity-driven TMAO cellular release, we measured platelet AANAT and ASMT activities in the same platelet samples and found that both activities decreased with decreasing osmolarities (Figure 3E). Since natremia is not a direct measurement of osmolarity, and since diluting Tyrode solution decreased both sodium concentration and osmolarity, we tested the impact of osmolarity on TMAO release by incubating platelets in Tyrode solution prepared with sodium concentrations similar to those of diluted Tyrode (130 mM, 123 mM, and 119 mM corresponding to Tyrode solution at 300 mOsm/L, 285 mOsm/L, and 275 mOsm/L) and adjusted osmolarity to 300 mOsm/L by adding TMG. Under such conditions, TMAO release was significant but markedly reduced when compared to diluted Tyrode solution (Figure 3F), suggesting that osmolarity was the main driver for TMAO release, although natremia had a modest effect. Consequently, the reduced TMAO release had no impact on platelet PST-P activity, unlike diluted Tyrode solution (Figure 3G). Taken together, these results suggest that hypoosmolarity is responsible for TMAO release from platelets and that individuals with ASD have hypotonic hyponatremia in most instances.

TMAO, transport, and signaling

In addition to its chaperoning role on soluble proteins, TMAO has membrane-rigidifying properties similar to cholesterol.[18] Taking

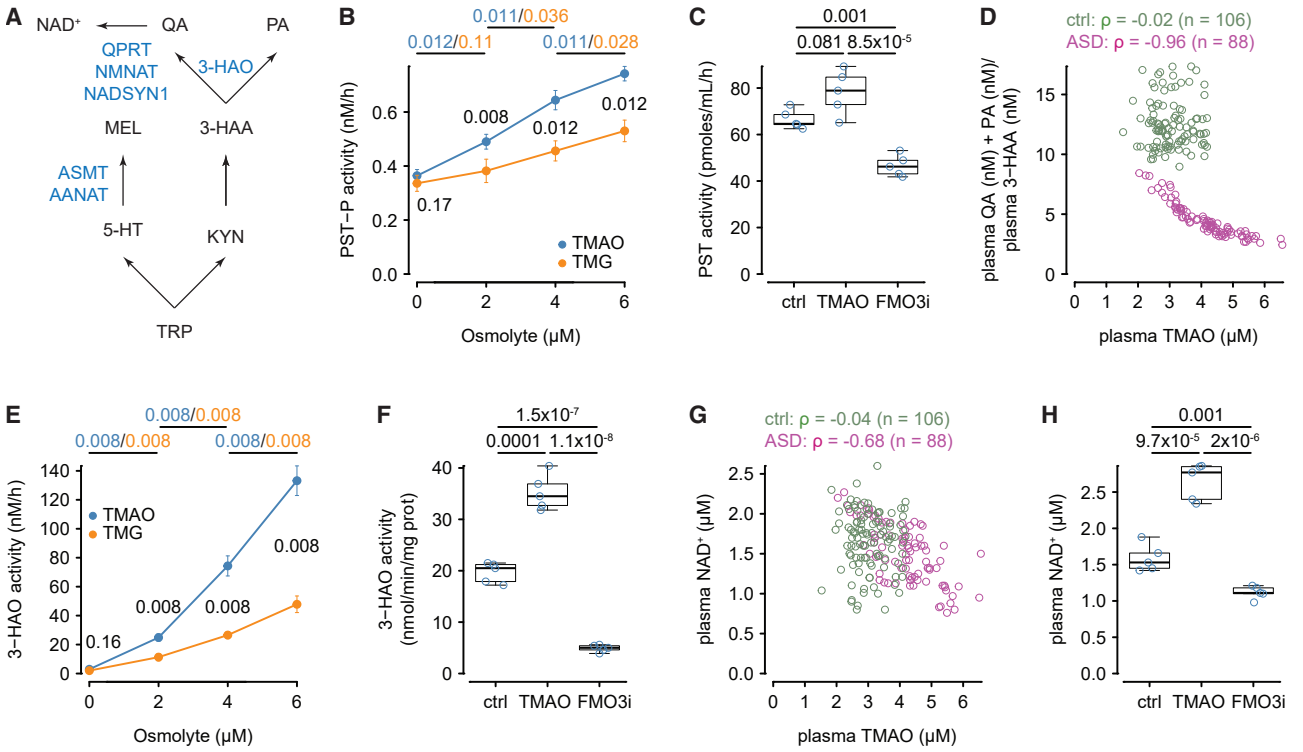

Figure 2. TMAO chaperones numerous enzymatic activities

(A) Simplified schematic representation of tryptophan (TRP) metabolism relevant for the study. MEL, melatonin; KYN, kynurenine, 3-HAA, 3-hydroxyanthranilic acid, QA, quinolinic acid, PA, picolinic acid, NAD^+, nicotinamide dinucleotide. Enzymes are indicated in blue: 3-HAO, 3-hydroxyanthranilate oxidase; AANAT, arylkylamine N-acetyltransferase; ASMT, acetylserotonin O-methyltransferase; NMNAT, nicotinamide nucleotide adenylyl transferase; NADSYN1, glutamine-dependent NAD^+ synthetase; and QPRT, quinolinate phosphoribosyl transferase.

(B) Activity of recombinant human phenol-specific phenol sulphotransferase (PST-P) with respect to TMAO (blue) and trimethyl glycine (TMG, orange) concentration (n = 5 per osmolyte concentration).

(C) Platelet PST activity measured in control mice, that successively received TMAO and FMO3 inhibitor (n = 5, see STAR Methods).

(D) Relationship between plasma TMAO concentration and 3-hydroxyanthranilate oxidase (3-HAO) activity estimated by the QA + PA/3-HAA ratio in controls and individuals with ASD.

(E) Activity of recombinant human 3-HAO with respect to TMAO (blue) and trimethyl glycine (TMG, orange) concentration (n = 5 per osmolyte concentration).

(F) Liver 3-HAO activity measured in control mice that successively received TMAO and FMO3 inhibitor (n = 5, see STAR Methods).

(G) Relationship between plasma TMAO and NAD^+ in controls and individuals with ASD.

(H) Plasma NAD^+ measured in control mice, that successively received TMAO and FMO3 inhibitor (n = 5, see STAR Methods).

Data are presented as mean ± SD (B and E) or as median and interquartile range along with individual datapoints (C, F, and H). Intergroup comparisons were performed using the Kruskal-Wallis test followed by the Wilcoxon sum-rank test corrected for multiple comparisons (B and E). Within-group comparisons were performed using repeated-measure ANOVA on log-transformed data followed by the Tukey HSD test (C, F, and H). Correlations (D and G) were calculated using Spearman's correlation coefficient (ρ). The corresponding p values are presented in Table S1. The number of individuals for each correlation is indicated on each plot.

advantage of the platelet model described previously, we evaluated the functional impact of intracellular TMAO depletion on the organic cation transporter 2 (OCT2, SLC22A2) and the vasopressin (AVP) receptor 1A (V1aR), which have relevance in ASD and psychiatric disorders.[32,33] Both proteins are present at the plasma membrane of platelets and require cholesterol for high-affinity binding of their ligands.[34,35] First, we incubated control human platelets in Tyrode solutions at different osmolarities with the pan-OCT inhibitor, decynium-22 (D22), and found a decrease in D22 binding with decreasing osmolarity (Figure 4A). *In vivo*, we also found a decrease in D22 binding in the hippocampus of developmental hyperserotonemia (DHS) rats, a model of ASD[36] (Figure 4B). To functionally test a deficit in OCT-2 transport, we measured the transport of 1-methyl-4-phenyl pyridinium (MPP^+) in the same setting and found a decrease in MPP^+ uptake (Figure 4A). We next investigated the binding of AVP to V1aR (the sole AVP receptor present in platelets[37]). In platelet samples from our cohort, we found a lower AVP binding in platelets from individuals with ASD than in controls (Figure 4C) despite similar V1aR protein levels (Figure 4D). Furthermore, AVP binding but not V1aR levels decreased with osmolarity in platelets from healthy subjects incubated in Tyrode solutions of varying osmolarities (Figure 4E). This decrease in AVP binding was associated with an overall decrease in IP_3 production, even when IP_3 production was expressed relatively to AVP binding when osmolarity

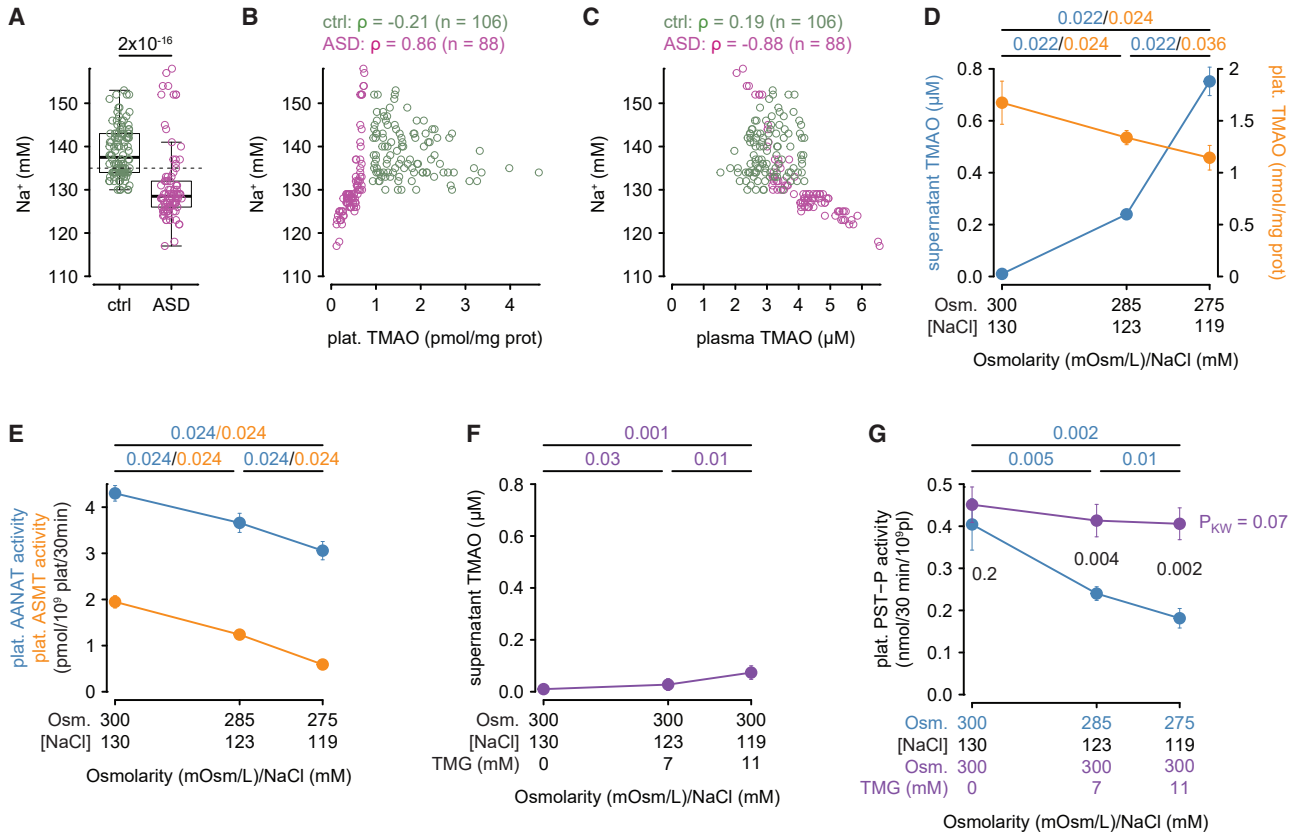

Figure 3. Osmolarity drives TMAO efflux

(A) Natremia of controls (n = 106) and individuals with ASD (n = 88). The dotted line indicates the lower limit of the reference range.

(B) Relationship between plasma TMAO concentration and natremia in controls and individuals with ASD.

(C) Relationship between platelet TMAO concentration and natremia in controls and individuals with ASD.

(D) Tyrode (blue) and platelet (orange) TMAO concentrations measured in control human platelets incubated in Tyrode solutions of varying osmolarity (n = 5 per condition).

(E) Platelet ANAAT (blue) and ASMT (orange) activities measured in human platelets incubated in Tyrode solutions of varying osmolarity (n = 5 per condition).

(F) Tyrode TMAO concentration measured in control human platelets with decreasing sodium concentration with osmolarity adjusted with trimethyl glycine (TMG).

(G) Platelet PST-P activity measured in control human platelets incubated in Tyrode solutions of varying osmolarity (blue) or in hyponatremic Tyrode with osmolarity adjusted with trimethyl glycine (TMG) (purple, n = 5 per condition).

Data are presented as mean ± SD (D–G) or as median and interquartile range along with individual datapoints (A). Intergroup comparisons were performed using the Wilcoxon sum-rank test (A) or the Kruskal-Wallis test followed by the Wilcoxon sum-rank test corrected for multiple comparisons (D–G). Correlations (B and C) were calculated using Spearman's correlation coefficient (ρ). The corresponding p values are presented in Table S1. The number of individuals for each correlation is indicated on each plot.

reached 275 mOsm/L (Figure 4F). These results are consistent with the results of a recent small clinical trial that found that intranasal AVP administration to children with ASD was more beneficial to children with the highest pre-treatment AVP blood levels, suggesting that AVP receptors could be less functional.[33] Taken together, these results strongly suggest that TMAO also influences transport across the plasma membrane as well as GPCR affinity and signaling.

Restoration of natraemia by urea in young DHS rats

We next hypothesized that restoring fluid/electrolyte balance in ASD using a salt-sparing diuretic should correct TMAO compartmentalization and alleviate the associated biochemical burden. To this end, we used the DHS rat model of ASD[36] (Figure 5A) and urea, as it is already clinically approved for the treatment of acute and chronic hyponatraemia.[38,39] Importantly, DHS rats shared numerous biochemical alterations found in individuals with ASD from the cohort: (1) hyperserotonemia (Figure 5B) as previously described,[36] (2) moderate hyponatremia (<130 mM, Figure 5C), (3) lower platelet and higher plasma TMAO levels (Figures 5D and 5E), and (4) lower plasma levels of melatonin (Figure 5F) and NAD^+ (Figure 5G). Young DHS rats were administered 0.5 g/kg/day urea subcutaneously for five days from PND21 to PND25 using an osmotic pump (Figure 5A). At PND33, urea had restored TMAO compartmentalization, and all the biochemical parameters tested were restored to control levels (Figures 5B–5G).

From a behavioral standpoint, at PND33, DHS rats exhibited a decrease in sociability using the three-chamber test for sociability and social preference (Figures 6A and 6B), an increase in anxiety

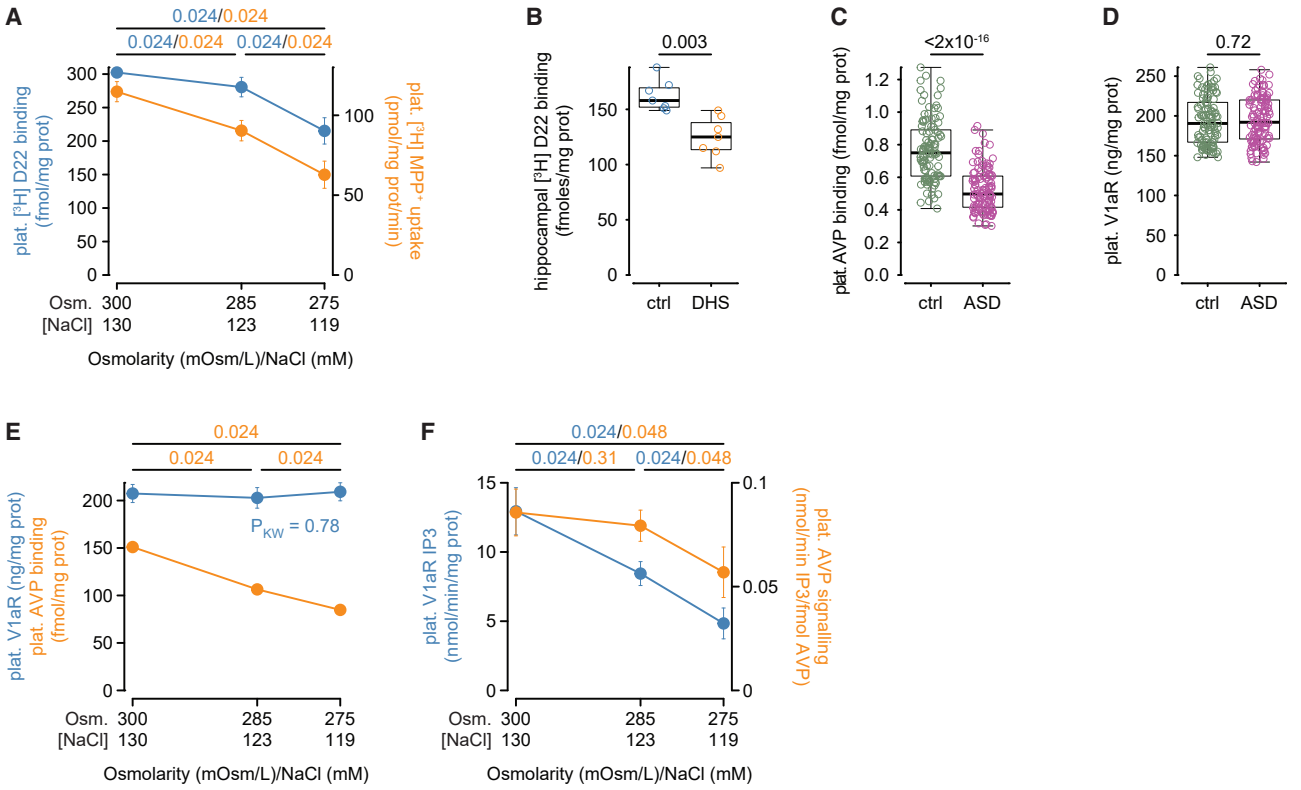

Figure 4. Impact of TMAO on transport and signaling

(A) [3H]-D22 binding (blue) and [3H]-MPP+ uptake (orange) measured in human platelets incubated in Tyrode solutions of varying osmolarity (n = 5 per condition).

(B) [3H]-D22 binding on the hippocampus of control and DHS rats (n = 7 per condition).

(C) AVP binding on platelets of controls (n = 106) and individuals with ASD (n = 88).

(D) Platelet V1aR concentrations in platelets of controls (n = 106) and individuals with ASD (n = 88).

(E) Platelet V1aR concentrations (blue) and AVP bindings (orange) measured in human platelets incubated in Tyrode solutions of varying osmolarity (n = 5 per condition).

(F) Platelet IP3 produced by V1aR after incubation with AVP (blue) and relative to AVP binding (orange) activities measured in human platelets incubated in Tyrode solutions of varying osmolarity (n = 5 per condition).

Data are presented as mean ± SD (A, E, and F) or as median and interquartile range along with individual datapoints (B–D). Intergroup comparisons were performed using the Wilcoxon sum-rank test (B–D) or the Kruskal-Wallis test followed by the Wilcoxon sum-rank test corrected for multiple comparisons (A, E, and F).

using the elevated plus maze (Figures 6C and 6D), an increase in locomotion in the open field tests (Figures 6E and 6F), and an increase in repetitive tasks using the spontaneous alternation test (Figure 6G). Urea administration markedly improved all behavioral parameters tested (Figures 6A–6G), rescuing at least 60% of the DHS phenotypes. When the same rats were re-evaluated at PND60-64 and PND90-94, all biochemical parameters except natremia and all behavioral parameters progressively reverted toward levels observed in untreated DHS rats (Figure S3). Altogether, these results show that the administration of urea in a young rat model of ASD restored TMAO compartmentalization, which was associated with the normalization of biochemical parameters and a broad improvement in behavior.

Restoration of osmolarity/natraemia by urea in adult DHS rats

As ASD is not restricted to children, we also tested urea in three-month-old DHS rats, that is, adult DHS rats, which exhibited similar biochemical and behavioral alteration than young DHS rats (Figure S4A). Urea normalized natremia (Figure S4B) and markedly improved TMAO compartmentalization (Figure S4C). Plasma NAD^+ levels (Figure S4D) were restored to control values, but whole-blood 5-HT (Figure S4E) and plasma melatonin levels (Figure S4F) were only partially yet significantly restored toward normal values. From a behavioral standpoint, urea significantly improved most parameters (Figures S4G–S4M). However, only sociability (Figures S4G and S4H) and general locomotion (Figure S4K) improved by more than 30%, while other parameters improved marginally (Figures S4I, S4J, S4L, and S4M). Altogether, these results show that the administration of urea in an adult rat model of ASD mainly restored TMAO compartmentalization, although its impact on biochemical and behavioral parameters was less remarkable than in young animals.

DISCUSSION

This study suggests that TMAO miscompartmentalization drives most biochemical and behavioral alterations in ASD. TMAO

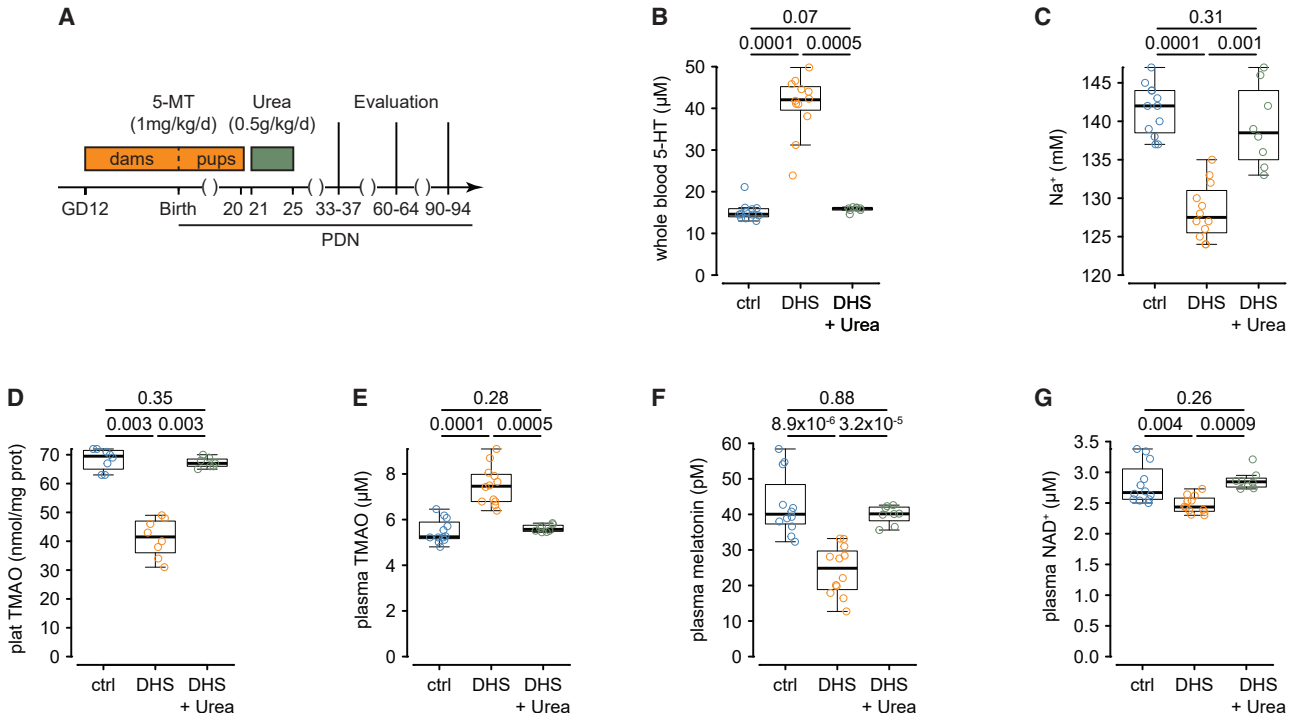

Figure 5. Effects of urea on biochemical parameters in young DHS rats

(A) Schematic representation of the experimental protocol (5-MT: 5-methoxytryptamine).

(B–G) Whole-blood serotonin (5-HT, B), Natremia (C), platelet (D), plasma TMAO (E), plasma melatonin (F), and NAD^+ (G) concentrations in control rats (n = 12, blue), DHS rats (n = 12, orange), and DHS rats treated with urea at PDN21-PDN25 (n = 8, green). Platelet TMAO was measured in 8 rats per group. Measurements were assessed at PDN33. Data are presented as interquartile range along with individual datapoints. Intergroup comparisons were performed using the Kruskal-Wallis test followed by the Wilcoxon sum-rank test corrected for multiple comparisons.

miscompartmentalization appears mainly driven by blood hypoosmolarity, which is pharmacologically actionable, and we established a proof of concept that the salt-sparing diuretic (urea) corrected TMAO miscompartmentalization and significantly improved biochemical and behavioral impairments in a rat model of ASD. Overall, this study posits intracellular TMAO deficit as a prevalent and major component of ASD pathophysiology and cellular physiology in general.

From a pathophysiological standpoint, lower intracellular TMAO levels observed in all individuals with ASD translated into elevated plasma TMAO levels. Such elevation in plasma TMAO levels has already been described in ASD,[25] suggesting that these findings are not restricted to our cohort. Of note, the difference in slope observed between controls and individuals with ASD for platelet/plasma TMAO concentrations (Figure 1F) may reflect that in individuals with ASD hypoosmolarity provokes an intracellular decrease in TMAO, which in turn reduced OCT-2 activity, the transporter responsible for TMAO cellular uptake.[40] TMAO miscompartmentalization was correlated with hyponatraemia, although *ex vivo* data and previously published data[30,31] suggest that hypoosmolarity is responsible for TMAO miscompartmentalization. Although all these measurements were performed in the blood, experimental hypotonic hyponatraemia caused cerebrospinal osmotic imbalance,[41] suggesting that osmolarity is also altered in the brain of individuals with ASD and is in line with the higher extra-axial cerebrospinal fluid (CSF) volume in ASD.[42] Therefore, it is likely that central TMAO miscompartmentalization parallels peripheral TMAO miscompartmentalization.

Our findings suggest that ASD is characterized by alterations in fluid/electrolyte homeostasis, resulting in TMAO miscompartmentalization, hence physiological imbalance. Yet, TMAO miscompartmentalization is *per se* not causative of ASD, as patients with primary trimethylaminuria (*FMO3* mutation) do not exhibit any ASD-like phenotype. However, TMAO intracellular depletion becomes critical in the context of serotonergic overstimulation by 5-MT (DHS rats). Interestingly, depletion or enhancement of 5-HT signaling has been associated with ASD,[43] suggesting that any alteration of the serotonergic system could be a common cause of ASD, especially in idiopathic cases. Therefore, we speculate that various mechanisms could provoke the deregulation of the serotonergic system, which in turn causes alteration in brain development and maturation, resulting in part by an impairment in fluid/electrolyte homeostasis; the latter possibly resulting in alterations of the development/maturation of the hypothalamus/pituitary/adrenal axis (Figure 7). Consequently, TMAO would become miscompartmentalized, resulting in the alteration of numerous enzymatic activities that affect various metabolisms that may contribute to most of the ASD-related and peripheral symptoms. As the correction of

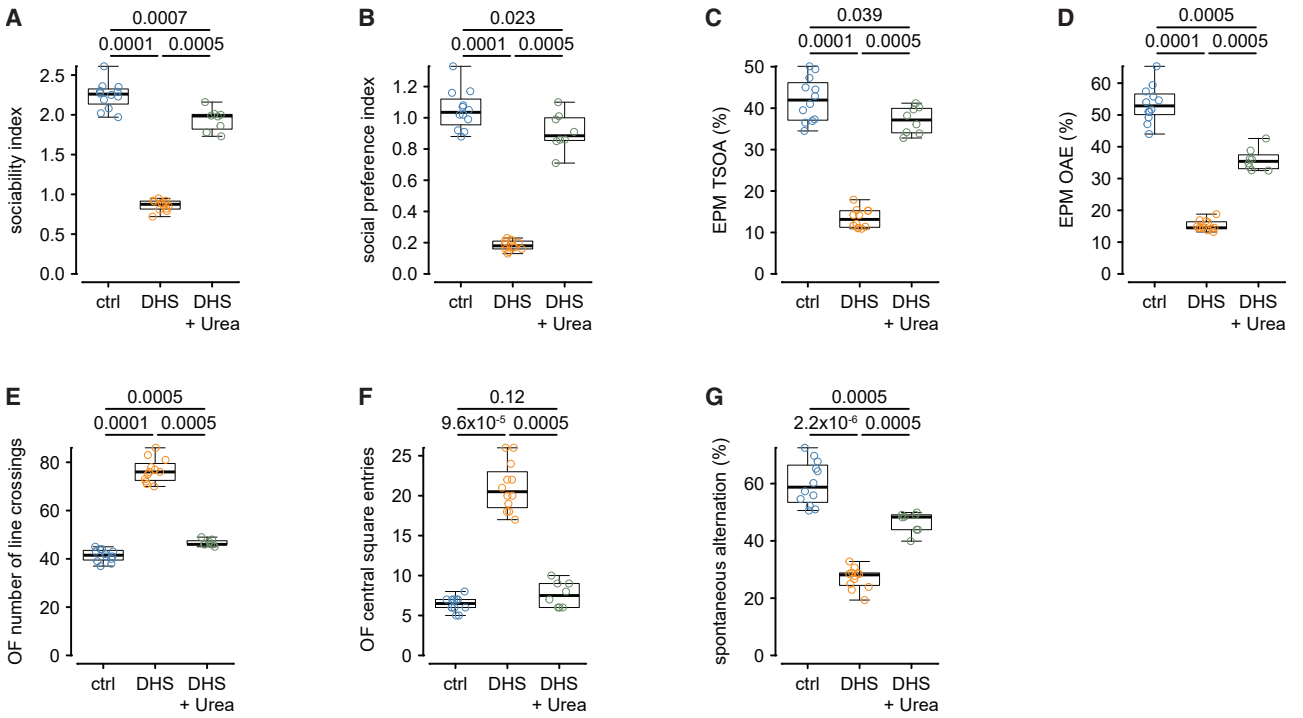

Figure 6. Effects of urea on behavioral parameters in young DHS rats

Sociability index (A), social preference index (B), time spent in the open arm (TSOA), C) and the number of open arm entries (OAE), (D) in the elevated plus maze (EPM), the number of line crossing (E) and the number of central square entry (F) in the open field (OF), and the % of spontaneous alternation (G) in control rats (n = 12, blue), DHS rats (n = 12, orange) and DHS rats treated with urea (n = 8, green). All behavioral testing were performed at PDN33. Data are presented as interquartile range along with individual datapoints. Intergroup comparisons were performed using the Kruskal-Wallis test followed by the Wilcoxon sum-rank test corrected for multiple comparisons.

TMAO miscompartmentalization by urea improved all behavioral symptoms in a rat model of ASD, we propose that the initial deregulation of the serotonergic system, in itself, may have mild behavioral consequences and that positive and negative reinforcements improve or worsen initial symptoms, TMAO miscompartmentalization being a major negative reinforcement (Figure 7).

From a therapeutic perspective, osmolarity can be readily corrected by dietary intake, such as salts.[44] However, dietary intake is non-existent during sleep. This suggests that the negative impact of TMAO miscompartmentalization resets every sleep cycle, which prompts a therapeutic intervention to correct fluid/electrolyte imbalance appropriately. In that regard, urea is a salt-sparing diuretic that is clinically approved for the acute[38] and chronic[39] treatment of hyponatremia. Consequently, urea provokes hemoconcentration without salt loss capable of restoring osmolarity and TMAO compartmentalization. Administration of urea showed major benefits in young DHS rats, whose age equivalence in humans (2–3 years old)[45] conveniently fits within the time frame of ASD diagnosis.[46] Moreover, DHS rats shared strong behavioral and phenotypic resemblance with the individuals with ASD from our cohort, suggesting potential transferability to humans. However, the phenotypic reversal observed after urea withdrawal advocates for the chronic administration of urea and indicates that urea only palliates to fluid/electrolyte imbalance and not its cause. In adult rats, the results were less spectacular, possibly due to differences in neuroplasticity,[45] which suggest that restoring urea treatment could improve post-natal cerebral development in children with ASD. Nevertheless, the biochemical improvements observed in adult rats treated with urea still warrant testing in adults with ASD to alleviate the biochemical burden ASD is associated with. Interestingly, urea is not the first diuretic to be tested in ASD. The loop diuretic bumetanide has shown promising results[47,48] for the treatment of ASD, although a recent phase 3 clinical trial failed to show efficacy.[49] Unlike urea, loop diuretics provoke the elimination of both water and sodium, with water loss exceeding that of salt, only resulting in partial hemoconcentration. Nevertheless, these data reinforce hypoosmolarity as a therapeutic target in ASD and posit urea as a better diuretic candidate than loop diuretic to treat ASD. Finally, these results suggest that loop diuretics act via a partial restoration of fluid/electrolyte homeostasis rather than a sole improvement in GABAergic signaling.

More broadly, our results show that TMAO is important, yet not essential, in cell physiology. Based on our data, TMAO appears to chaperone homodimeric interactions (sulphotransferase activities) and protein complexes (melatonin synthesis) and play a major role in membrane fluidity, hence GPCR signaling (V1aR) and transport (OCT-2), under physiological conditions.

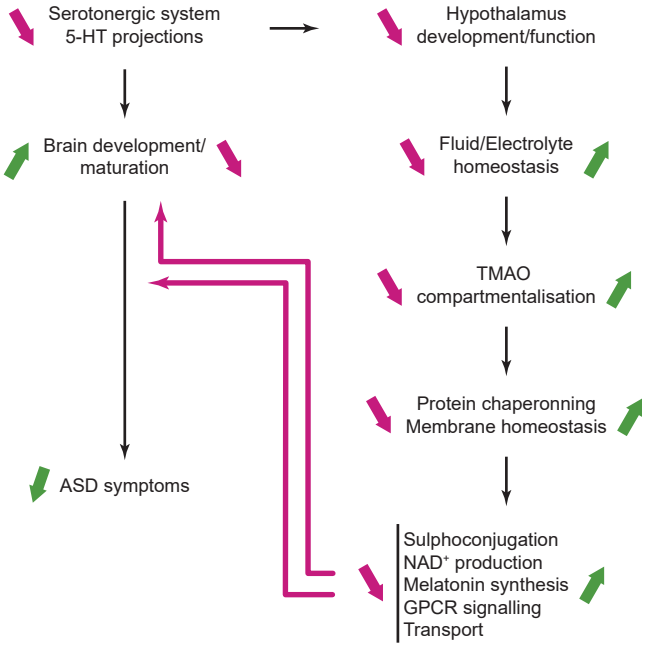

Figure 7. Tentative model involving osmolarity and inappropriate TMAO compartmentalization in the pathophysiology of ASD
In the model, magenta indicates ASD and green the effect of urea.

However, it should be noted that TMAO does not always have a positive effect on proteins,[50,51] indicating that TMAO homeostasis is important. A recent study has shown that only ~5% of cellular water content was free and suggested that the main impact of change in electric charge by post-translational modification was to modify the behavior of water molecules around a protein.[52] Importantly, TMAO does not physically interact with either proteins[53–55] or lipids[20,21,56] but rather interacts with the surrounding water molecules.[55] Furthermore, the high TMAO dipole moment modifies water distribution around it.[57] Therefore, given the ubiquitous nature of TMAO-water interactions, we anticipate TMAO to impact a vast majority of proteins and lipids in the cell.

In conclusion, TMAO appears to be a major modulator of cell physiology and suggests its miscompartmentalization as a major worsening factor in ASD. Given the phenotypic similarities between DHS rats and individuals with ASD, urea- or any salt-sparing diuretics offer a promising therapeutic option for ASD that warrants carefully designed clinical trials in humans to address the safety, acceptability, and dosing in this context, taking into account the heterogeneity of ASD.

Limitations of the study

A limitation of this study is the size of the cohort and the fact that ASD was determined based on the revised version of the of the fourth edition of the Diagnostic and Statistical Manual of Mental Disorders (DSM-IV-TR), which may less reflect the heterogeneity of ASD than current description. However, the fact that elevated TMAO was observed in a different cohort of ASD suggest that this may be a commonality in ASD individuals, although further study are required to evaluate this aspect. A second limitation of the study is the use of the DHS rat model. Although this model recapitulated the biochemical and behavioral phenotype of the individuals with ASD of the cohort, they may not reflect the entire spectrum of ASD.

RESOURCE AVAILABILITY

Lead contact

Request for further information and resources should be directed to and will be fulfilled by the lead contact, Nicolas Vodovar (nicolas.vodovar@inserm.fr).

Materials availability

This study did not generate any new materials.

Data and code availability

- The datasets generated and analyzed have been deposited at Harvard Dataverse: https://doi.org/10.7910/DVN/4FQZRA.
- This study did not generate any code.
- Any additional information required to reanalyze the data reported in this paper is available from the lead contact upon request.

ACKNOWLEDGMENTS

We thank individuals with ASD and their families and the controls who accepted to participate in this study. We would like to thank Professors Marion Leboyer and Richard Delorme for providing human biological samples and Dr Michel Vodovar for critical discussions. This work is dedicated to the memory of Mosé Da Prada (1930–1995), whose pioneering interest in osmolarity laid the foundation for this work. This work was supported by funding from Institut National de la Santé et Recherche Médicale and Université Paris Cité.

AUTHOR CONTRIBUTIONS

Conceptualization, N.V. and J.-M.L.; methodology and experimentation, N.V. and J.-M.L.; data analysis, N.V.; writing original manuscript, N.V.; review and editing of the manuscript, J.-M.L.; funding acquisition, N.V.

DECLARATION OF INTERESTS

The authors declare no competing interests.

STAR★METHODS

Detailed methods are provided in the online version of this paper and include the following:

- KEY RESOURCES TABLE
- EXPERIMENTAL MODEL AND STUDY PARTICIPANT DETAILS
  - Human cohort
  - Mouse model
  - Developmental hyperserotonemia (DHS) rat model
  - Ethical statement
- METHOD DETAILS
  - Osmolarity experiments
  - Natremia
  - Immunoprecipitation/mass spectrometry
  - TMA, and TMAO quantification by LC/MS
  - TMG quantification by LC/MS
  - Other biochemical measurements
  - Enzymatic activities
  - *In vitro* enzymatic reactions
  - Binding and uptake experiments
  - Behavioral analyses
- QUANTIFICATION AND STATISTICAL ANALYSIS

SUPPLEMENTAL INFORMATION

Supplemental information can be found online at https://doi.org/10.1016/j.isci.2026.117276.

Received: September 24, 2025
Revised: May 4, 2026
Accepted: August 5, 2026
Published: August 24, 2026

REFERENCES

1. American Psychiatric Association (2013). Diagnostic and Statistical Manual of Mental Disorders. DSM-5. https://doi.org/10.1176/appi.books.9780890425596.
2. Miles, J.H. (2011). Autism spectrum disorders–a genetics review. Genet. Med. *13*, 278–294. https://doi.org/10.1097/GIM.0b013e3181ff67ba.
3. Doi, M., Li, M., Usui, N., and Shimada, S. (2022). Genomic Strategies for Understanding the Pathophysiology of Autism Spectrum Disorder. Front. Mol. Neurosci. *15*, 930941. https://doi.org/10.3389/fnmol.2022.930941.
4. Rolland, T., Cliquet, F., Anney, R.J.L., Moreau, C., Traut, N., Mathieu, A., Huguet, G., Duan, J., Warrier, V., Portalier, S., et al. (2023). Phenotypic effects of genetic variants associated with autism. Nat. Med. *29*, 1671–1680. https://doi.org/10.1038/s41591-023-02408-2.
5. Safadi, J.M., Quinton, A.M.G., Lennox, B.R., Burnet, P.W.J., and Minichino, A. (2022). Gut dysbiosis in severe mental illness and chronic fatigue: a novel trans-diagnostic construct? A systematic review and meta-analysis. Mol. Psychiatry *27*, 141–153. https://doi.org/10.1038/s41380-021-01032-1.
6. Yap, C.X., Henders, A.K., Alvares, G.A., Wood, D.L.A., Krause, L., Tyson, G.W., Restuadi, R., Wallace, L., McLaren, T., Hansell, N.K., et al. (2021). Autism-related dietary preferences mediate autism-gut microbiome associations. Cell *184*, 5916–5931.e17. https://doi.org/10.1016/j.cell.2021.10.015.
7. Pagan, C., Benabou, M., Leblond, C., Cliquet, F., Mathieu, A., Lemière, N., Goubran-Botros, H., Delorme, R., Leboyer, M., Callebert, J., et al. (2021). Decreased phenol sulfotransferase activities associated with hyperserotonemia in autism spectrum disorders. Transl. Psychiatry *11*, 23. https://doi.org/10.1038/s41398-020-01125-5.
8. Pagan, C., Goubran-Botros, H., Delorme, R., Benabou, M., Lemière, N., Murray, K., Amsellem, F., Callebert, J., Chaste, P., Jamain, S., et al. (2017). Disruption of melatonin synthesis is associated with impaired 14-3-3 and miR-451 levels in patients with autism spectrum disorders. Sci. Rep. *7*, 2096. https://doi.org/10.1038/s41598-017-02152-x.
9. Launay, J.M., Delorme, R., Pagan, C., Callebert, J., Leboyer, M., and Vodovar, N. (2023). Impact of IDO activation and alterations in the kynurenine pathway on hyperserotonemia, NAD(+) production, and AhR activation in autism spectrum disorder. Transl. Psychiatry *13*, 380. https://doi.org/10.1038/s41398-023-02687-w.
10. Loo, R.L., Chan, Q., Nicholson, J.K., and Holmes, E. (2022). Balancing the Equation: A Natural History of Trimethylamine and Trimethylamine-N-oxide. J. Proteome Res. *21*, 560–589. https://doi.org/10.1021/acs.jproteome.1c00851.
11. Fahnert, B. (2012). Using folding promoting agents in recombinant protein production: a review. Methods Mol. Biol. *824*, 3–36. https://doi.org/10.1007/978-1-61779-433-9_1.
12. Cho, I.C., and Swaisgood, H. (1973). Factors affecting tetramer dissociation of rabbit muscle lactate dehydrogenase and reactivity of its sulfhydryl groups. Biochemistry *12*, 1572–1577. https://doi.org/10.1021/bi00732a017.
13. Kumari, K., Singh, K.S., Singh, K., Bakhshi, R., and Singh, L.R. (2022). TMAO to the rescue of pathogenic protein variants. Biochim. Biophys. Acta Gen. Subj. *1866*, 130214. https://doi.org/10.1016/j.bbagen.2022.130214.
14. Miller, A.L., Elam, W.A., Johnson, B.H., Khan, S.H., Kumar, R., and Thompson, E.B. (2017). Restored mutant receptor:Corticoid binding in chaperone complexes by trimethylamine N-oxide. PLoS One *12*, e0174183. https://doi.org/10.1371/journal.pone.0174183.
15. Yancey, P.H., and Somero, G.N. (1979). Counteraction of urea destabilization of protein structure by methylamine osmoregulatory compounds of elasmobranch fishes. Biochem. J. *183*, 317–323. https://doi.org/10.1042/bj1830317.
16. Yancey, P.H., and Siebenaller, J.F. (1999). Trimethylamine oxide stabilizes teleost and mammalian lactate dehydrogenases against inactivation by hydrostatic pressure and trypsinolysis. J. Exp. Biol. *202*, 3597–3603. https://doi.org/10.1242/jeb.202.24.3597.
17. Lambert, D., Leipply, D., and Draper, D.E. (2010). The osmolyte TMAO stabilizes native RNA tertiary structures in the absence of Mg2+: evidence for a large barrier to folding from phosphate dehydration. J. Mol. Biol. *404*, 138–157. https://doi.org/10.1016/j.jmb.2010.09.043.
18. Nandi, S., Pyne, A., Layek, S., Arora, C., and Sarkar, N. (2021). The Dietary Nutrient Trimethylamine N-Oxide Affects the Phospholipid Vesicle Membrane: Probable Route to Adverse Intake. J. Phys. Chem. Lett. *12*, 12411–12418. https://doi.org/10.1021/acs.jpclett.1c03201.
19. Higgins, T., Chaykin, S., Hammond, K.B., and Humbert, J.R. (1972). Trimethylamine N-oxide synthesis: a human variant. Biochem. Med. *6*, 392–396. https://doi.org/10.1016/0006-2944(72)90025-7.
20. Maiti, A., and Daschakraborty, S. (2021). Effect of TMAO on the Structure and Phase Transition of Lipid Membranes: Potential Role of TMAO in Stabilizing Cell Membranes under Osmotic Stress. J. Phys. Chem. B *125*, 1167–1180. https://doi.org/10.1021/acs.jpcb.0c08335.
21. Manisegaran, M., Bornemann, S., Kiesel, I., and Winter, R. (2019). Effects of the deep-sea osmolyte TMAO on the temperature and pressure dependent structure and phase behavior of lipid membranes. Phys. Chem. Chem. Phys. *21*, 18533–18540. https://doi.org/10.1039/c9cp03812d.
22. Koeth, R.A., Wang, Z., Levison, B.S., Buffa, J.A., Org, E., Sheehy, B.T., Britt, E.B., Fu, X., Wu, Y., Li, L., et al. (2013). Intestinal microbiota metabolism of L-carnitine, a nutrient in red meat, promotes atherosclerosis. Nat. Med. *19*, 576–585. https://doi.org/10.1038/nm.3145.
23. Tang, W.H.W., Wang, Z., Levison, B.S., Koeth, R.A., Britt, E.B., Fu, X., Wu, Y., and Hazen, S.L. (2013). Intestinal microbial metabolism of phosphatidylcholine and cardiovascular risk. N. Engl. J. Med. *368*, 1575–1584. https://doi.org/10.1056/NEJMoa1109400.
24. Zhu, W., Gregory, J.C., Org, E., Buffa, J.A., Gupta, N., Wang, Z., Li, L., Fu, X., Wu, Y., Mehrabian, M., et al. (2016). Gut Microbial Metabolite TMAO Enhances Platelet Hyperreactivity and Thrombosis Risk. Cell *165*, 111–124. https://doi.org/10.1016/j.cell.2016.02.011.
25. Quan, L., Yi, J., Zhao, Y., Zhang, F., Shi, X.T., Feng, Z., and Miller, H.L. (2020). Plasma trimethylamine N-oxide, a gut microbe-generated phosphatidylcholine metabolite, is associated with autism spectrum disorders. Neurotoxicology *76*, 93–98. https://doi.org/10.1016/j.neuro.2019.10.012.
26. Obsil, T., Ghirlando, R., Klein, D.C., Ganguly, S., and Dyda, F. (2001). Crystal structure of the 14-3-3zeta:serotonin N-acetyltransferase complex. a role for scaffolding in enzyme regulation. Cell *105*, 257–267. https://doi.org/10.1016/s0092-8674(01)00316-6.
27. Li, H., Nguyen, H.H., Ogorzalek Loo, R.R., Campuzano, I.D.G., and Loo, J.A. (2018). An integrated native mass spectrometry and top-down proteomics method that connects sequence to structure and function of macromolecular complexes. Nat. Chem. *10*, 139–148. https://doi.org/10.1038/nchem.2908.
28. Chen, Y.L., Tang, L.C., Zhou, W., Sun, X., Lai, Z.Z., Xu, S., Cai, K., Shi, Y., Zhao, R., Zhou, X.Y., et al. (2026). Endometrial stromal cell-derived TMAO sustains decidualization to prevent recurrent spontaneous abortion. Cell Metab. *38*, 316–330.e8. https://doi.org/10.1016/j.cmet.2025.11.014.
29. Pagan, C., Delorme, R., Callebert, J., Goubran-Botros, H., Amsellem, F., Drouot, X., Boudebesse, C., Le Dudal, K., Ngo-Nguyen, N., Laouamri,

H., et al. (2014). The serotonin-N-acetylserotonin-melatonin pathway as a biomarker for autism spectrum disorders. Transl. Psychiatry *4*, e479. https://doi.org/10.1038/tp.2014.120.

30. Koomoa, D.L., Musch, M.W., MacLean, A.V., and Goldstein, L. (2001). Volume-activated trimethylamine oxide efflux in red blood cells of spiny dogfish (Squalus acanthias). Am. J. Physiol. Regul. Integr. Comp. Physiol. *281*, R803–R810. https://doi.org/10.1152/ajpregu.2001.281.3.R803.
31. MacLellan, R.J., Tunnah, L., Barnett, D., Wright, P.A., MacCormack, T., and Currie, S. (2015). Chaperone roles for TMAO and HSP70 during hyposmotic stress in the spiny dogfish shark (Squalus acanthias). J. Comp. Physiol. B *185*, 729–740. https://doi.org/10.1007/s00360-015-0916-6.
32. Daws, L.C. (2021). Organic Cation Transporters in Psychiatric Disorders. Handb. Exp. Pharmacol. *266*, 215–239. https://doi.org/10.1007/164_2021_473.
33. Parker, K.J., Oztan, O., Libove, R.A., Mohsin, N., Karhson, D.S., Sumiyoshi, R.D., Summers, J.E., Hinman, K.E., Motonaga, K.S., Phillips, J.M., et al. (2019). A randomized placebo-controlled pilot trial shows that intranasal vasopressin improves social deficits in children with autism. Sci. Transl. Med. *11*, eaau7356. https://doi.org/10.1126/scitranslmed.aau7356.
34. Hörmann, S., Gai, Z., Kullak-Ublick, G.A., and Visentin, M. (2020). Plasma Membrane Cholesterol Regulates the Allosteric Binding of 1-Methyl-4-Phenylpyridinium to Organic Cation Transporter 2 (SLC22A2). J. Pharmacol. Exp. Ther. *372*, 46–53. https://doi.org/10.1124/jpet.119.260877.
35. Wiegand, V., and Gimpl, G. (2012). Specification of the cholesterol interaction with the oxytocin receptor using a chimeric receptor approach. Eur. J. Pharmacol. *676*, 12–19. https://doi.org/10.1016/j.ejphar.2011.11.041.
36. McNamara, I.M., Borella, A.W., Bialowas, L.A., and Whitaker-Azmitia, P.M. (2008). Further studies in the developmental hyperserotonemia model (DHS) of autism: social, behavioral and peptide changes. Brain Res. *1189*, 203–214. https://doi.org/10.1016/j.brainres.2007.10.063.
37. Launay, J.M., Vittet, D., Vidaud, M., Rondot, A., Mathieu, M.N., Lalau-Keraly, C., Cantau, B., and Chevillard, C. (1987). V1a-vasopressin specific receptors on human platelets: potentiation by ADP and epinephrine and evidence for homologous down-regulation. Thromb. Res. *45*, 323–331. https://doi.org/10.1016/0049-3848(87)90221-0.
38. Decaux, G., Kengne, F., Couturier, B., Vandergheynst, F., Musch, W., and Soupart, A. (2014). Actual Therapeutic Indication of an Old Drug: Urea for Treatment of Severely Symptomatic and Mild Chronic Hyponatremia Related to SIADH. J. Clin. Med. *3*, 1043–1049. https://doi.org/10.3390/jcm3031043.
39. Rondon-Berrios, H. (2020). Urea for Chronic Hyponatremia. Blood Purif. *49*, 212–218. https://doi.org/10.1159/000503773.
40. Teft, W.A., Morse, B.L., Leake, B.F., Wilson, A., Mansell, S.E., Hegele, R.A., Ho, R.H., and Kim, R.B. (2017). Identification and Characterization of Trimethylamine-N-oxide Uptake and Efflux Transporters. Mol. Pharm. *14*, 310–318. https://doi.org/10.1021/acs.molpharmaceut.6b00937.
41. Melton, J.E., and Nattie, E.E. (1983). Brain and CSF water and ions during dilutional and isosmotic hyponatremia in the rat. Am. J. Physiol. Regul. Integr. Comp. Physiol. *244*, R724–R732. https://doi.org/10.1152/ajpregu.1983.244.5.R724.
42. Shen, M.D., Nordahl, C.W., Li, D.D., Lee, A., Angkustsiri, K., Emerson, R.W., Rogers, S.J., Ozonoff, S., and Amaral, D.G. (2018). Extra-axial cerebrospinal fluid in high-risk and normal-risk children with autism aged 2-4 years: a case-control study. Lancet Psychiatry *5*, 895–904. https://doi.org/10.1016/S2215-0366(18)30294-3.
43. Garbarino, V.R., Gilman, T.L., Daws, L.C., and Gould, G.G. (2019). Extreme enhancement or depletion of serotonin transporter function and serotonin availability in autism spectrum disorder. Pharmacol. Res. *140*, 85–99. https://doi.org/10.1016/j.phrs.2018.07.010.
44. Good, P. (2011). Do salt cravings in children with autistic disorders reveal low blood sodium depleting brain taurine and glutamine? Med. Hypotheses *77*, 1015–1021. https://doi.org/10.1016/j.mehy.2011.08.038.
45. Semple, B.D., Blomgren, K., Gimlin, K., Ferriero, D.M., and Noble-Haeusslein, L.J. (2013). Brain development in rodents and humans: Identifying benchmarks of maturation and vulnerability to injury across species. Prog Neurobiol *106–107*, 1–16. https://doi.org/10.1016/j.pneurobio.2013.04.001.
46. Hyman, S.L., Levy, S.E., Myers, S.M., Council On Children With Disabilities, S.O.D., Kuo, D.Z., Apkon, S., Davidson, L.F., Ellerbeck, K.A., Foster, J.E., Noritz, G.H., et al. (2020). Identification, Evaluation, and Management of Children With Autism Spectrum Disorder. Pediatrics *145*, e20193447. https://doi.org/10.1542/peds.2019-3447.
47. Lemonnier, E., Villeneuve, N., Sonie, S., Serret, S., Rosier, A., Roue, M., Brosset, P., Viellard, M., Bernoux, D., Rondeau, S., et al. (2017). Effects of bumetanide on neurobehavioral function in children and adolescents with autism spectrum disorders. Transl. Psychiatry *7*, e1056. https://doi.org/10.1038/tp.2017.10.
48. Sprengers, J.J., van Andel, D.M., Zuithoff, N.P.A., Keijzer-Veen, M.G., Schulp, A.J.A., Scheepers, F.E., Lilien, M.R., Oranje, B., and Bruining, H. (2021). Bumetanide for Core Symptoms of Autism Spectrum Disorder (BAMBI): A Single Center, Double-Blinded, Participant-Randomized, Placebo-Controlled, Phase-2 Superiority Trial. J. Am. Acad. Child Adolesc. Psychiatry *60*, 865–876. https://doi.org/10.1016/j.jaac.2020.07.888.
49. Fuentes, J., Parellada, M., Georgoula, C., Oliveira, G., Marret, S., Crutel, V., Albarran, C., Lambert, E., Pénélaud, P., Ravel, D., and Ben Ari, Y. (2023). Bumetanide oral solution for the treatment of children and adolescents with autism spectrum disorder: Results from two randomized phase III studies. Autism Res. *16*, 2021–2034. https://doi.org/10.1002/aur.3005.
50. Buawangpong, N., Pinyopornpanish, K., Siri-Angkul, N., Chattipakorn, N., and Chattipakorn, S.C. (2022). The role of trimethylamine-N-Oxide in the development of Alzheimer's disease. J. Cell. Physiol. *237*, 1661–1685. https://doi.org/10.1002/jcp.30646.
51. Sackett, D.L. (1997). Natural osmolyte trimethylamine N-oxide stimulates tubulin polymerization and reverses urea inhibition. Am. J. Physiol. Regul. Integr. Comp. Physiol. *273*, R669–R676. https://doi.org/10.1152/ajpregu.1997.273.2.R669.
52. Watson, J.L., Seinkmane, E., Styles, C.T., Mihut, A., Krüger, L.K., McNally, K.E., Planelles-Herrero, V.J., Dudek, M., McCall, P.M., Barbiero, S., et al. (2023). Macromolecular condensation buffers intracellular water potential. Nature *623*, 842–852. https://doi.org/10.1038/s41586-023-06626-z.
53. Zou, Q., Bennion, B.J., Daggett, V., and Murphy, K.P. (2002). The molecular mechanism of stabilization of proteins by TMAO and its ability to counteract the effects of urea. J. Am. Chem. Soc. *124*, 1192–1202. https://doi.org/10.1021/ja004206b.
54. Hu, C.Y., Lynch, G.C., Kokubo, H., and Pettitt, B.M. (2010). Trimethylamine N-oxide influence on the backbone of proteins: an oligoglycine model. Proteins *78*, 695–704. https://doi.org/10.1002/prot.22598.
55. Canchi, D.R., Jayasimha, P., Rau, D.C., Makhatadze, G.I., and Garcia, A.E. (2012). Molecular mechanism for the preferential exclusion of TMAO from protein surfaces. J. Phys. Chem. B *116*, 12095–12104. https://doi.org/10.1021/jp304298c.
56. Sukenik, S., Dunsky, S., Barnoy, A., Shumilin, I., and Harries, D. (2017). TMAO mediates effective attraction between lipid membranes by partitioning unevenly between bulk and lipid domains. Phys. Chem. Chem. Phys. *19*, 29862–29871. https://doi.org/10.1039/c7cp04603k.
57. Kuroki, N., Uchino, Y., Funakura, T., and Mori, H. (2022). Electronic fluctuation difference between trimethylamine N-oxide and tert-butyl alcohol in water. Sci. Rep. *12*, 19417. https://doi.org/10.1038/s41598-022-24049-0.
58. Launay, J.M., Geoffroy, C., Mutel, V., Buckle, M., Cesura, A., Alouf, J.E., and Da Prada, M. (1992). One-step purification of the serotonin transporter located at the human platelet plasma membrane. J. Biol. Chem. *267*, 11344–11351. https://doi.org/10.1016/s0021-9258(19)49916-x.

59. Launay, J.M., Geoffroy, C., Costa, J.L., and Alouf, J.E. (1984). Purified -SH-activated toxins (streptolysin O, alveolysin): new tools for determination of platelet enzyme activities. Thromb. Res. *33*, 189–196. https://doi.org/10.1016/0049-3848(84)90179-8.

60. Geoffroy, C., and Alouf, J.E. (1988). Molecular cloning and characterization of Bacillus alvei thiol-dependent cytolytic toxin expressed in Escherichia coli. J. Gen. Microbiol. *134*, 1961–1970. https://doi.org/10.1099/00221287-134-7-1961.

61. Launay, J.M., and Alouf, J.E. (1979). Biochemical and ultrastructural study of the disruption of blood platelets by streptolysin O. Biochim. Biophys. Acta Biomembr. *556*, 278–291. https://doi.org/10.1016/0005-2736(79)90048-8.

62. Fuertig, R., Ceci, A., Camus, S.M., Bezard, E., Luippold, A.H., and Hengerer, B. (2016). LC-MS/MS-based quantification of kynurenine metabolites, tryptophan, monoamines and neopterin in plasma, cerebrospinal fluid and brain. Bioanalysis *8*, 1903–1917. https://doi.org/10.4155/bio-2016-0111.

63. Trammell, S.A.J., Schmidt, M.S., Weidemann, B.J., Redpath, P., Jaksch, F., Dellinger, R.W., Li, Z., Abel, E.D., Migaud, M.E., and Brenner, C. (2016). Nicotinamide riboside is uniquely and orally bioavailable in mice and humans. Nat. Commun. *7*, 12948. https://doi.org/10.1038/ncomms12948.

64. Namboodiri, M.A.A., Nakai, C., and Klein, D.C. (1979). Effects of selected treatments on stability and activity of pineal serotonin N-acetyltransferase. J. Neurochem. *33*, 807–810. https://doi.org/10.1111/j.1471-4159.1979.tb05229.x.

65. Axelrod, J., Wurtman, R.J., and Snyder, S.H. (1965). Control of Hydroxyindole O-Methyltransferase Activity in the Rat Pineal Gland by Environmental Lighting. J. Biol. Chem. *240*, 949–954. https://doi.org/10.1016/s0021-9258(17)45266-5.

66. Ben-Abdallah, M., Bondet, V., Fauchereau, F., Béguin, P., Goubran-Botros, H., Pagan, C., Bourgeron, T., and Bellalou, J. (2011). Production of soluble, active acetyl serotonin methyl transferase in Leishmania tarentolae. Protein Expr. Purif. *75*, 114–118. https://doi.org/10.1016/j.pep.2010.07.011.

67. Ferry, G., Ubeaud, C., Dauly, C., Mozo, J., Guillard, S., Berger, S., Jimenez, S., Scoul, C., Leclerc, G., Yous, S., et al. (2004). Purification of the recombinant human serotonin N-acetyltransferase (EC 2.3.1.87): further characterization of and comparison with AANAT from other species. Protein Expr. Purif. *38*, 84–98. https://doi.org/10.1016/j.pep.2004.07.004.

68. Tugaeva, K.V., Remeeva, A., Gushchin, I., Cooley, R.B., and Sluchanko, N.N. (2020). Design, expression, purification and crystallization of human 14-3-3zeta protein chimera with phosphopeptide from proapoptotic protein BAD. Protein Expr. Purif. *175*, 105707. https://doi.org/10.1016/j.pep.2020.105707.

69. Walker, R.F., Friedman, D.W., and Jimenez, A. (1983). A modified enzymatic-isotopic microassay for serotonin (5HT) using 5HT-N-acetyltransferase partially purified from Drosophila. Life Sci. *33*, 1915–1924. https://doi.org/10.1016/0024-3205(83)90676-8.

70. Nishikawa, M., Masuyama, Y., Nunome, M., Yasuda, K., Sakaki, T., and Ikushiro, S. (2018). Whole-cell-dependent biosynthesis of sulfo-conjugate using human sulfotransferase expressing budding yeast. Appl. Microbiol. Biotechnol. *102*, 723–732. https://doi.org/10.1007/s00253-017-8621-x.

71. Falany, C.N., and Kerl, E.A. (1990). Sulfation of minoxidil by human liver phenol sulfotransferase. Biochem. Pharmacol. *40*, 1027–1032. https://doi.org/10.1016/0006-2952(90)90489-8.

72. Malherbe, P., Köhler, C., Da Prada, M., Lang, G., Kiefer, V., Schwarcz, R., Lahm, H.W., and Cesura, A.M. (1994). Molecular cloning and functional expression of human 3-hydroxyanthranilic-acid dioxygenase. J. Biol. Chem. *269*, 13792–13797. https://doi.org/10.1016/s0021-9258(17)36717-0.

73. Vittet, D., Rondot, A., Cantau, B., Launay, J.M., and Chevillard, C. (1986). Nature and properties of human platelet vasopressin receptors. Biochem. J. *233*, 631–636. https://doi.org/10.1042/bj2330631.

74. Gould, G.G., Barba-Escobedo, P.A., Horton, R.E., and Daws, L.C. (2022). High Affinity Decynium-22 Binding to Brain Membrane Homogenates and Reduced Dorsal Camouflaging after Acute Exposure to it in Zebrafish. Front. Pharmacol. *13*, 841423. https://doi.org/10.3389/fphar.2022.841423.

75. Delorme, R., Betancur, C., Callebert, J., Chabane, N., Laplanche, J.L., Mouren-Simeoni, M.C., Launay, J.M., and Leboyer, M. (2005). Platelet serotonergic markers as endophenotypes for obsessive-compulsive disorder. Neuropsychopharmacology *30*, 1539–1547. https://doi.org/10.1038/sj.npp.1300752.

76. Cesura, A.M., Ritter, A., Picotti, G.B., and Da Prada, M. (1987). Uptake, release, and subcellular localization of 1-methyl-4-phenylpyridinium in blood platelets. J. Neurochem. *49*, 138–145. https://doi.org/10.1111/j.1471-4159.1987.tb03405.x.

77. Mony, T.J., Lee, J.W., Dreyfus, C., DiCicco-Bloom, E., and Lee, H.J. (2016). Valproic Acid Exposure during Early Postnatal Gliogenesis Leads to Autistic-like Behaviors in Rats. Clin. Psychopharmacol. Neurosci. *14*, 338–344. https://doi.org/10.9758/cpn.2016.14.4.338.

78. Mirza, R., and Sharma, B. (2019). Benefits of Fenofibrate in prenatal valproic acid-induced autism spectrum disorder related phenotype in rats. Brain Res. Bull. *147*, 36–46. https://doi.org/10.1016/j.brainresbull.2019.02.003.

79. Kumar, H., and Sharma, B. (2016). Memantine ameliorates autistic behavior, biochemistry & blood brain barrier impairments in rats. Brain Res. Bull. *124*, 27–39. https://doi.org/10.1016/j.brainresbull.2016.03.013.

80. Mony, T.J., Hong, M., and Lee, H.J. (2018). Empathy Study in Rodent Model of Autism Spectrum Disorders. Psychiatry Investig. *15*, 104–110. https://doi.org/10.30773/pi.2017.06.20.

81. Madden, A.M.K., and Zup, S.L. (2014). Effects of developmental hyperserotonemia on juvenile play behavior, oxytocin and serotonin receptor expression in the hypothalamus are age and sex dependent. Physiol. Behav. *128*, 260–269. https://doi.org/10.1016/j.physbeh.2014.01.036.

82. Lai, M.C., Lombardo, M.V., and Baron-Cohen, S. (2014). Autism. Lancet *383*, 896–910. https://doi.org/10.1016/S0140-6736(13)61539-1.

83. Mirza, R., and Sharma, B. (2018). Selective modulator of peroxisome proliferator-activated receptor-alpha protects propionic acid induced autism-like phenotypes in rats. Life Sci. *214*, 106–117. https://doi.org/10.1016/j.lfs.2018.10.045.

84. Veenstra-VanderWeele, J., Muller, C.L., Iwamoto, H., Sauer, J.E., Owens, W.A., Shah, C.R., Cohen, J., Mannangatti, P., Jessen, T., Thompson, B.J., et al. (2012). Autism gene variant causes hyperserotonemia, serotonin receptor hypersensitivity, social impairment and repetitive behavior. Proc. Natl. Acad. Sci. USA *109*, 5469–5474. https://doi.org/10.1073/pnas.1112345109.

85. Cuevas-Olguin, R., Roychowdhury, S., Banerjee, A., Garcia-Oscos, F., Esquivel-Rendon, E., Bringas, M.E., Kilgard, M.P., Flores, G., and Atzori, M. (2017). Cerebrolysin prevents deficits in social behavior, repetitive conduct, and synaptic inhibition in a rat model of autism. J. Neurosci. Res. *95*, 2456–2468. https://doi.org/10.1002/jnr.24072.

STAR★METHODS

KEY RESOURCES TABLE

REAGENT or RESOURCE	SOURCE	IDENTIFIER
Antibodies		
Human anti-p31T-AANAT	Merck	AB-5467
anti-ASMT	EpiGentek	A72945
Biological samples		
Human EDTA plasma samples	NCT02628808	NCT02628808
Chemicals, peptides, and recombinant proteins		
5-methoxytryptamine	Sigma Aldrich	286583
Urea	Sigma Aldrich	U5128
[H-3] MPP+ acetate	Tritec	RCTT0970
Critical commercial assays		
Melatonin Radioimmunoassay	Novolytix	RK-MEL2
14-3-3 Pro ELISA kit	MyBioSource	#MBS269690
Inositol 1,4,5 Triphosphate RIA Kit	Perkin Elmer	NEK-064
Deposited data		
Datasets	Harvard Dataverse	https://doi.org/10.7910/DVN/4FQZRA
Experimental models: Organisms/strains		
FVB/N male mice	Charles River	Strain code: 207
Sprague-Dawley female rats	Charles River	Sprague-Dawley Rats (CD® IGS)
Software and algorithms		
R statistical software version 4.0.3	https://www.r-project.org/	N/A

EXPERIMENTAL MODEL AND STUDY PARTICIPANT DETAILS

Human cohort

The cohort used has already been described.[7,9] It consisted of 88 individuals with ASD and 106 neurotypic controls. Clinical evaluations and blood sampling of individuals with ASD (diagnosed according to DSM-IVTR) and control individuals from the general population investigated for genetics and blood biochemistry have previously been detailed.[7,29] Venous blood samples were collected after a 48-h diet that excluded important sources of serotonin and tryptophan.

Individuals with ASD were hospitalized for 48h, and blood samples were collected on the last morning, on waking, before any food or fluid intake. For controls, fasting blood samples were collected.

All blood samples were collected between 8:30 and 10:00 into tubes containing 109 mM sodium citrate (Greiner Bio-One) with a 9:1 blood-to-anticoagulant ratio. After removing 0.5 mL of whole blood (for serotonin measurement), the remainder was centrifuged at 1,000 *x* g for 10 min to obtain platelet-rich plasma, which was then centrifuged at 3,000 *x* g for 15 min to isolate platelets and obtain platelet-poor plasma. Importantly, the time between blood sampling and platelet/plasma isolation was less than 1 h. Whole blood, platelets, and plasma were aliquoted into barcode-labeled cryovials and stored at −80°C until investigations. All samples for ASD individuals and controls were collected during the same period. All measurements were performed blinded.

Mouse model

Wild-type male FVB/N mice were from Charles River and housed in light- (on from 08:00 – 20:00 h) and temperature (22°C)-controlled testing rooms, with food and water available *ad libitum*. Blood samples were obtained from the submandibular (facial) vein at baseline, after administration of 50 μg/kg TMAO, and after administration of 3 mg/kg of the FMO3 inhibitor phenylthiourea. The same animals were used throughout the experiment. A one-week wash-out period was allowed between the administration of exogenous TMAO and FMO3i phenylthiourea, once confirmed that plasma TMAO levels returned to baseline levels. Males were selected to reflect the strong sex-ratio bias observed in ASD.

Developmental hyperserotonemia (DHS) rat model

The developmental hyperserotonaemia (DHS) rat model for ASD was performed as previously described.[36] Nulliparous Sprague-Dawley female rats (180–220 g) were from Charles River and housed in metabolic cages, in light- (on from 08:00 – 20:00 h) and temperature (22°C)-controlled testing rooms, with food and water available *ad libitum*. They were mated overnight, and fertilization was determined using a vaginal smear; this day was considered gestational day 0 (GD0). Eight pregnant females were administered a single subcutaneous dose (1.0 mg/kg of body weight) of 5-methoxytryptamine (5-MT, Sigma Aldrich St. Louis MO) daily from GD12 to parturition, and five pregnant females received the vehicle in equal volumes on the same days. Upon parturition (postnatal day [PND] 0), litters were culled to five males and five females. Male pups exposed to 5-MT *in utero* were further administered 5-MT by intraperitoneal injection from PND0 to PND20, to induce DHS. Similarly, pups only exposed to the vehicle prenatally were administered the vehicle in equal volumes. Rejection from the dams was prevented by smearing the pups with urine collected from the metabolic cage after each manipulation. At PND21 (young rats) or PND91 (adult rats), 0.5 g/kg body weight/day urea (Sigma-Aldrich) was administered subcutaneously using an Alzet osmotic pump (Durect Corp., Cupertino, CA) for 5 days. Males were selected to reflect the strong sex-ratio bias observed in ASD.

Ethical statement

This study was approved by the local ethics committee (Comité de Protection des Personnes Ile de France IX, ref: 2008-A00019-46) and was performed according to the current revision of the Helsinki Declaration. Written informed consent was obtained after oral and written information from all participants, their parents or legal guardians. Animal care and experimental procedures complied with the European Communities Council Directive (CEE 86/609/EEC), EU Directive 2017/32/EU, and French Departmental Direction of Animal Protection (2019-11 #1027).

METHOD DETAILS

Osmolarity experiments

For osmolarity experiments, human platelets from healthy donors were isolated after blood collection on pre-chilled Vacutainer tubes containing sodium citrate as described above. The platelet pellet was resuspended in a Tyrode-Tris buffer, pH 7.40, 290–310 mOsm/L (NaCl 130 mM; KCl 5.6 mM; Tris 12.4 mM; Na_4EDTA 2.1 mM; NaH_2PO_4 0.9 mM; sucrose 13.1 mM; and dextrose 11.1 mM), which was selected as the most efficient for the study of 5-HT uptake and platelet physiology on isolated platelets.[58] Tyrode solution was diluted with water to decrease osmolarity to 285 and 275 mOsm/L. When testing the impact of natremia, Tyrode solution was prepared with varying amounts of NaCl corresponding to the final NaCl concentration at 300, 285, and 275 mOsm.

Natremia

Natremia was measured on fresh plasma at the time of collection by potentiometry on an Abbott Architect c8000 (Abbott Laboratories, Abbott Park, IL, USA).

Immunoprecipitation/mass spectrometry

Platelet samples from healthy individuals were obtained as described above. Platelet lysis was achieved by -SH-activated toxin treatment.[59] 150 hemolytic units of alveolysin (purified as in[60]) per 1.5×10^9 platelets (equivalent to about 375 ng or 6 pmol of protein) were added (10:1) to platelet suspensions at 4°C and the suspensions were warmed to 37°C for enzyme measurement. This amount of toxin binds to platelets at 4°C and elicits complete lysis at 37°C since about 16 molecules of toxin are sufficient to lyse one human platelet.[61] Immunoprecipitations were performed using human anti-p31T-AANAT (ref: AB-5467, Merck, Darmstadt, Germany; RRID:AB_2219739) or anti-ASMT (ref: A72945, EpiGentek, Farmingdale, NY, USA). GC-MS analysis was carried out on a TRACE GC 2000 Series (ThermoQuest CE Instruments, Austin TX, USA) gas chromatograph, interfaced with GCQ Plus (ThermoQuest) mass detector with ion trap analyzer, operating in EI mode (70 eV). The capillary GC column was an OV-1 (30 m × 0.25 mm ID, OV-1 bonded, 0.25 μm film thickness ref. 1105–2502 105, Ohio Valley Specialty Co, Marietta OH, USA). Helium was the carrier gas at a flow rate of 1.0 mL/min. A temperature program was adopted: initial temperature was 40°C (hold time: 5 min), then ramp by 10 C/min to 220°C (hold time: 5 min). The temperatures of the transfer line and ionization source were maintained at 250°C and 200°C respectively. The GC was operated in split-less mode; the injector base temperature was set at 250°C. The mass spectra were recorded in full scan mode (30–200 amu) to collect the total ion current (TIC) chromatograms. Quantitation was carried out by using the extracted ion chromatograms (XIC) by selecting qualifier and quantifier fragment ions of the studied analytes. Standard TMAO and the concentrated eluates were run under the same conditions.

TMA, and TMAO quantification by LC/MS

Twenty-five μL of plasma, platelet lysate or whole blood and 300 μL of acetonitrile:methanol:water (5:4:1; v/v:v) containing the internal standards (IS) d9-TMAO and d9-TMA for quantification were mixed and vigorously vortexed for 20 s. The samples were re-equilibrated on ice for 30 min and centrifuged for 10 min at 25,100×g at 4°C. The supernatant was then transferred into a specific vial before liquid chromatography-mass spectrometry (LC-MS) analysis. Matrix-matched calibration curves were generated using a human control plasma pool spiked with the standards. The concentration range of the calibration curves was 0–250 μM. An

ultra-high-performance LC system coupled with a 6490 triple-quadrupole mass spectrometer (QqQ, Agilent Technologies) using an electrospray as an ion source (LC-ESI-QqQ) working in positive mode was used to analyze the extracts. An ACQUITY UPLC BEHHILIC column (1.7 mm, 2.1 × 150 mm, Waters) and a gradient mobile phase containing water with 50 mM ammonium acetate (phase A) and acetonitrile (phase B) were used to perform the chromatographic separation. The gradient was as follows: for 0.5 min, isocratic at 75% B; from 0.5 to 2 min, reduced to 65% B; from 2 to 2.1 min, decreased to 45% B; from 2.1 to 3.9 min, maintained at 45% B; from 3.9 to 4 min, hiked up to 75% B; and, finally, until 5.5 min, the column was equilibrated at 75% B. The flow throughout this process was 0.6 mL/min. Two hundred microliters of plasma extract were injected into the LC system. The mass spectrometer conditions were: a drying gas temperature of 280°C and a sheath gas temperature of 400°C; source and sheath gas flows of 20 and 12 L/min, respectively; a nebulizer flow of 60 psi; a nozzle voltage of 500 V; a capillary voltage of 2500 V; and iFunnel and HRF values of 110 and 80 V, respectively. The QqQ worked in the multiple reaction monitoring (MRM) mode and used predetermined transitions and collision energies (CE(V)) of 16 (transition 76 → 58) and 8 (transition 76 → 59) for TMAO, (transitions 60 → 44 and 60 → 52) for TMA and of 16 (transition 85 → 67) and 8 (transition 85 → 68), (transitions 69 → 53 and 69 → 60) for d9-TMAO and d9-TMA (ISs) respectively.

TMG quantification by LC/MS

Plasma or platelet lysate samples (10 μL) and 10 μL of IS solution (d9-TMG, 500 ng/mL) were put into a 1.5 mL Eppendorf tube. Then 200 μL of methanol was added and the mixture was vortex-mixed for 2 min, followed by centrifugated at 15,000 rpm at 4 °C for 5 min. The supernatant, transferred to another tube, was evaporated to dryness using a vacuum drying concentrator at 25 °C. Finally, the drying residue was dissolved in 100 μL of methanol-acetonitrile (25:75, *v*: *v*), followed by vortex-mixed for 2 min, and then centrifuged at 15000 rpm for 5 min. The corresponding supernatant was transferred to an auto-sampler vial with an insert (LVI, 150 μL, Waters) and 10 μL was injected into the UPLC–MS/MS system for analysis. The UPLC (Thermo Fisher Scientific Inc., Boston, USA) system was made up with Ultimate 3000 RSLC system equipped with binary pumps and S Surveyor autosampler (Thermo Fisher Scientific Inc., Boston, USA). The treated sample (10 μL) was injected to the system on a Waters Acquity BEH Amide (2.1 × 100 mm, 1.7 μm) column. The flow rate was set at 0.4 mL/min and composed of Water (A) (containing 10 mM ammonium formate, pH = 3.0) and acetonitrile (B) as the mobile phase. The condition of isocratic elution was set to 60% B and the total running time was 3 min. All the samples were kept in the auto-sampler at 10 °C.

The triple-quadrupole tandem mass spectrometric detection was performed on a TSQ Quantum Acess Max API mass spectrometer (Thermo Fisher Scientific Inc, Boston, USA) furnished with an electrospray ionization (ESI) interface. Under selected reactions monitoring (SRM), quantification was obtained using positive ion pairs at *m/z* transitions of *m/z* 118.1 → 58.3 for TMG, and *m/z* 127.1 → 67.2 for d9-TMG, respectively. The optimized parameters were as follows: heated capillary temperature: 350 °C; spray voltage: 3500 v; sheath gas (nitrogen): 30 psi; the auxiliary gas (nitrogen): 5 psi; the collision gas (argon): 1.5 mm Torr; the collision energy: 21 eV for TMG; 22 eV for d9-TMG. The data acquisition and procession was performed with the Thermo Scientific Xcalibur 2.0.7 SP1 data system.

Other biochemical measurements

Serotonin and kynurenine metabolites were measured by LC-MS/MS as previously described.[62] Melatonin was measured using a radioimmunoassay (ref: RK-MEL2, Novolytix, Switzerland) according to the manufacturer's instructions. NAD^+ concentrations were determined by LC-MS as described previously.[63] The amount of 14-3-3 proteins was determined using the commercial 14-3-3 Pro ELISA kit from MyBioSource (San Diego, CA, USA). The immunogen used to produce the antibodies is recombinant full-length human 14-3-3 γ. The kit has about 40% cross-reactivity with 14-3-3 ζ, ε, σ, τ (MyBioSource, personal communication).

Enzymatic activities

Platelet or tissue lysis was achieved by -SH-activated toxin treatment[59] as described above. Separate experiments showed that the addition of equivalent amounts of toxin to cells already disrupted by homogenization produced no change in the rates of enzyme activities measured at least in duplicate. Under the conditions employed here, enzyme rates were linear with time and with platelet protein concentrations ranging from 0.01 to 0.1 mg of protein per mL. PST (EC 2.8.2.1) activities were determined by radioenzymology using *p*-nitrophenol as the substrate for humans (PST-P) and mice (PST).[7] Measurement of AANAT activity[64] was performed at 37°C in 1.5 mL polypropylene microtubes. The reaction was started by the addition of enzyme preparation (25 μL) to 40 μL buffer containing 20 mM sodium citrate (pH 7.00), 300 mM NaCl, 1 mM EDTA, 0.05 mg/mL BSA, 50 nM [acetyl-^{3} H]-CoA, and 500 nM tryptamine. After 20 min the reaction was stopped by adding 1 mL of chloroform and vortexing the mixture. The reaction product, N-[^{3}H]-acetyl tryptamine, was extracted into the chloroform which was then washed once with 0.1 mL of 0.1 mM sodium phosphate buffer, pH 6.80. A 500 μL aliquot of the chloroform was then transferred to a scintillation vial. Three mL of scintillation fluid were added and the radioactivity was measured by a liquid scintillation counter (Beckman LS 6000SC).

The reaction mixtures for ASMT assay[65] contained in a final volume of 50 μL the following: N-acetylserotonin (1 mM), tissue homogenate (25 μL), and 0.1 mM S-[methyl-^{3}H]-adenosyl-L-methionine. Reactions were carried out in plastic Eppendorf tubes at 37°C for 30 min in 50 mM sodium phosphate buffer (pH 7.90). Reactions were stopped by the addition of 100 μL of 0.5 M borate buffer (pH 10.50) to the tubes. Blanks consisted of reaction mixtures minus N-acetylserotonin. One mL of chloroform was added.

The mixture was vortexed twice for 15 s to extract the product, [^{3}H]-melatonin, into the chloroform. The organic layer was washed once with borate buffer, and an aliquot (500 μL) was dried and its radioactivity measured. To verify that the activities measured in platelets reflect authentic AANAT and ASMT and not non-specific actions of other N-acetyltransferases and methyltransferases, si-RNA specific for each enzyme (SR300008 and SR300317, Origene; 1 nM final concentrations after transfection by the siTran 1.0 as recommended by Origene) were used. 3-HAO activity was determined by the decrease in 3-HK measured by LC-MS/MS[62] in 10 mM HEPES, pH 6.5, containing 0.3 mM $Fe(NH_4SO_4)_2$.

In vitro enzymatic reactions

Human recombinant AANAT, ASMT and 14-3-3ζ were purified as previously described[66–68] and mixed in 1:1:2 ratio in the presence of 10 nM 5-HT binoxalate in optimal conditions for melatonin production.[69] Human recombinant *SULT1A1* gene product (PST-P) was expressed in budding yeast[70] and purified as previously described.[71] PST-P activity was measured using *p*-nitrophenol as substrate.[7] Human recombinant 3-HAO was purified as previously described[72] and its activity was measured as described above.

Binding and uptake experiments

AVP binding on platelet membranes and D-22 binding on rat hippocampal membranes were performed as previously published[73,74] with 5 nM [^{3}H]AVP and 7.5 nM [^{3}H]D-22, respectively. Platelet IP_3 concentrations were measured radio-immunologically as described previously[75] except the TRK 1000 kit (Amersham) was replaced by the NEK 064 kit (PerkinElmer, Boston, MA, USA). The recovery was 90.1 ± 4.8% and the intra- and inter-assay coefficients of variations were 4.4% and 7%, respectively. Platelet MPP^+ uptake ([^{3}H]MPP^+ ref RCTT0970 from Tritec, Teufen, Switzerland) was performed as previously published.[76]

Behavioral analyses

All behavioral studies were conducted during the light phase, between 09:00 and 18:00 h, and were assessed by three independent observers blinded for the intervention; each data point corresponds to the median of the three independent measures (relative variation < 10%). To assess the impact of urea on DHS rats, animals were exposed to behavioral protocols on open field-spontaneous locomotory activity (PND33, PND60, PND90 in young rats and PDN103 for adult rats),[77] three-chambered social interaction–social behavior/interaction (PND34-35, PDN61-62, PDN91-92 for young rats and PDN104-105 for adult rats), y-maze–repetitive behavior (PND36, PND63, PND93 and PDN106 for adult rats)[78] and elevated plus maze (EPM)–anxiety (PND37, PND64, PND94 for young rats and PND107 for adult rats).[79] Animals were placed in the testing area 5 days before the beginning of the behavioral experiments. To reduce the chances of olfaction-related cues during testing, the test arena was cleaned with 70% v/v ethyl alcohol and dried between each consecutive trial.

Locomotor activity

Spontaneous increase in locomotion is extensively reported as one of the important features of the DHS model. This hyper-locomotion was measured using an open-field apparatus. The apparatus measured 90 cm × 90 cm with 50 cm high walls made of dark-colored wood. The animals (PND33, PND60, PND90 in young rats and PDN103 for adult rats) were introduced individually into the center of the arena for a single 10-min trial period.[80] The total number of line crossings and the total number of central square entries were recorded to assess changes in the locomotion of the animals.

Social behavior

Diminished and abnormal social interaction is a core phenotype of ASD, which may be mimicked by the DHS model.[81] This change in social behavior was assessed using the three-chambered social interaction test protocol (PND34-35, PDN61-62, PDN91-92 for young rats and PDN104-105 for adult rats).[78] The test arena measured 76 cm × 30 cm x 35 cm and was divided into three chambers with an access point between each chamber. Animals had free access to all the chambers and each trial began with the animal being placed in the central chamber. To encourage exploration of the side chambers, all animals were habituated to the apparatus for 5 min before initiation of the test trial. After ending of the habituation period, the rats were tested in the sociability phase lasting for 10 min. Animals to be placed under a wire cage were habituated to the wire cage for 30 min, 24 h before the beginning of the sociability phase. In the sociability phase, a stranger animal was placed under the wired cage in either (left or right) side chamber, while in the other chamber, an empty cage would be placed. To avoid side preferences, the placement of wired cages was randomized and the chamber with the stranger animal and the empty cage are referred to as the stranger chamber and the empty chamber, respectively. Upon conclusion of the sociability phase, the social preference phase was initiated 2 h after the last animal trial. In the social preference phase, each animal was allowed to explore the complete arena for 10 min. During this phase, the animal previously considered a stranger was now familiar and a new stranger animal was introduced into the previously empty cage. So, the two chambers now became the familiar chamber and the novel chamber. The time spent by test animals in both chambers containing the cages was measured. The sociability index (SI) and the social preference index (SPI) were calculated according to the following formula[79]: Sociability index = total time in the stranger chamber/total time in the empty chamber, and Sociability Preference Index (SPI) = total time in the novel chamber/total time in the familiar chamber, respectively.

Anxiety

Anxiety is the most common co-morbid trait expressed with ASD.[82] An elevated plus maze (EPM) is a commonly used apparatus to assess anxiety-like behavior in animal models of ASD. The EPM apparatus was made up of wood with four arms at 90° to each other. Two open arms and two closed arms were 50 × 10 cm in dimensions, enclosed by a 40 cm high wall. To facilitate exploration

of the maze, all animals were placed in a pre-test arena for 5 min each (PND37, PND64, PND94 for young rats and PND107 for adult rats). Soon after, the animals were transferred to the EPM placed 50 cm high from the ground. All animals were released in the center of the maze, pointing toward the open arm and entries along with the time spent in each arm were recorded for 5 min. The basis of this test is the conflict associated with the two parts of the maze, i.e., the open arms, which are aversive, bright and unprotected and the closed arms, which are covered, shadowy and protected. To this, the number of open arm entries and the closed arm entries, time spent in the open arm and time spent in the closed arm were measured to finally calculate % open arm entries and % open arm time, using the following formula[83]: % open arm entries (OAE) = 100 *x* number of entries in open arm/(closed arm entries + open arm entries) and % time spent in open arm (TSOA) = 100 *x* time spent in open arm/(time spent in open arm + time spent in the closed arm).

Repetitive behavior

One of the core diagnostic features of ASD is the presence of stereotypical or repetitive behavior; this key clinical feature is replicated by inducing DHS.[84] The extent of % spontaneous alteration is regarded as a measure of stereotypy or repetitive behavior in animals. A Y-maze apparatus was used to assess % spontaneous alterations.[85] The maze makes a Y shape, with three arms of equal length, each at an angle of 120° from the other. One of the arms was considered the start arm, and all animals were placed at the end of this arm, pointing toward the center of the maze. The animals were subjected to 8 min of testing in the Y-maze (PND36, PND63, PND93 and PND106 for adult rats). The exploration of three different arms in succession was considered as one alternation. Serial arm entries were observed for each animal to calculate % spontaneous alternations. The % spontaneous alternation can be calculated with the following formula: % Spontaneous alternation = 100 *x* total alternations/(total arm entries−2).

QUANTIFICATION AND STATISTICAL ANALYSIS

Data are represented as mean ± SD or median and interquartile range along with data dispersion, as appropriate. The number of biological objects, the test used, and the exact *p*-values are indicated in each panel in the legends to the figures. All the statistical analyses were performed using R statistical software (version 4.2.1). Data normality was assessed using the Shapiro-Wilk test. Data are presented as boxplots where the box represents the 25^{th} (Q1) and 75^{th} (Q2) percentile, the line in the box represents the median, and the whiskers represent Q1 - the interquartile range (IQR) and the 75^{th} percentile + IQR. Intergroup comparisons were performed using the Wilcoxon sum-rank test or the Kruskal-Wallis test followed by the Wilcoxon sum-rank test corrected for multiple comparisons (Holm). Longitudinal data were analyzed using repeated-measures ANOVA on log-transformed data followed by the Tukey Honest Statistical Significance Difference test. Correlations between variables were evaluated using Spearman's correlation coefficient (ρ). A p-value < 0.05 was considered significant, and exact p-values are reported unless $<2 \times 10^{-16}$. Statistical details for correlation, repeated-measure ANOVA, and Kruskal-Wallis tests are reported in Tables S1–S3, respectively.